Enhancements of Satellite Data Assimilation over Antarctica

Aurélie Bouchard, Florence Rabier, Vincent Guidard, Fatima Karbou

Enhancements of Satellite Data Assimilation over Antarctica

AURÉLIE BOUCHARD, FLORENCE RABIER, VINCENT GUIDARD, AND FATIMA KARBOU

CNRM-GAME, Météo-France, and CNRS, Toulouse, France

(Manuscript received 22 May 2009, in final form 4 December 2009)

ABSTRACT

The Concordiasi field experiment, which is taking place in Antarctica, involves the launching of radiosoundings and stratospheric balloons. One of the main goals of this campaign is the validation of the Infrared Atmospheric Sounding Interferometer (IASI) radiance assimilation. Prior to the campaign, it was necessary to improve satellite data assimilation at high latitudes. Two types of sensors, microwave and infrared, have been considered to help with this issue. A major problem associated with microwave satellite data is the calculation of the surface emissivity. An innovative approach, based on satellite observations, improves the surface emissivity modeling over land and sea ice within the constraints of the four-dimensional variational data assimilation (4D-VAR) system. With this new calculation of emissivity, it has been possible to include many more microwave observations during the assimilation. In this study, this method has been applied to high latitudes, after some adjustments have been made to assimilate additional Advanced Microwave Sounding Unit-A/B (AMSU-A/B) data over sea ice and snow. The use of additional data from IASI and the Atmospheric Infrared Sounder (AIRS) sensors over land and sea ice has also been tested. The use of the microwave and infrared data over this polar area has modified the dynamical and thermodynamical model fields such as the snow precipitation quantity. Additional data have been found to have a positive impact on the skill of a model specially tuned for Antarctica.

1. Introduction

From a climate change and chemical point of view, polar regions play a key role in the environment. From the conclusions of the most recent Intergovernmental Panel on Climate Change (IPCC; Solomon et al. 2007), relevant to this study, one can mention an increase of the mean sea level (from 0.1 to 0.2 cm), an increase of the global temperature (about 0.6 K), and a decrease of the snow cover and glacier extent (Jourdan 2007; Turner et al. 2005). Known since the 1980s (Semane 2008), ozone depletion is a key feature of today's Antarctica. It is governed by the atmospheric temperature and dynamical processes such as transport (Brewer–Dobson stratospheric circulation) and mixing. For both issues of climate change and of ozone destruction, an accurate knowledge of the atmosphere over Antarctica is required. The fourth International Polar Year (IPY), organized through the International Council for Science (ICSU) and the World Meteorological Organization (WMO), took place from March 2007 to March 2009. A wide range of research topics were examined during this period, such as changes about snow and ice (e.g., the evolution of the amount of snow cover, the changes in sea ice cover), and the global linkage between high and low latitudes (Nordeng et al. 2007). The Concordiasi project was launched in the framework of IPY (Rabier et al. 2007, 2010). One of the main aims of this project is to enhance the assimilation of satellite data, and in particular, of the Infrared Atmospheric Sounding Interferometer (IASI) data over Antarctica, so as to improve numerical weather prediction (NWP) and to help understand climate records through reanalysis. The project features three campaigns of observations, one during the austral spring 2008, the second in 2009 focusing on mesoscale studies, and the last one in 2010. Each campaign provides in situ validation data [radiosounding launches (2008), instrumented tower of 45 m (2009), stratospheric balloons (2010)]. This current study deals with the preparation of the campaign through state-of-the-art data assimilation over Antarctica.

High latitudes have specific features, such as a predominance of sea ice, ice sheet, and snow coverage. Pendlebury et al. (2003) has demonstrated that the quality

Corresponding author address: Florence Rabier, Météo France, 42 avenue Gaspard Coriolis, 31057 Toulouse, France.
E-mail: florence.rabier@meteo.fr

DOI: 10.1175/2009MWR3071.1

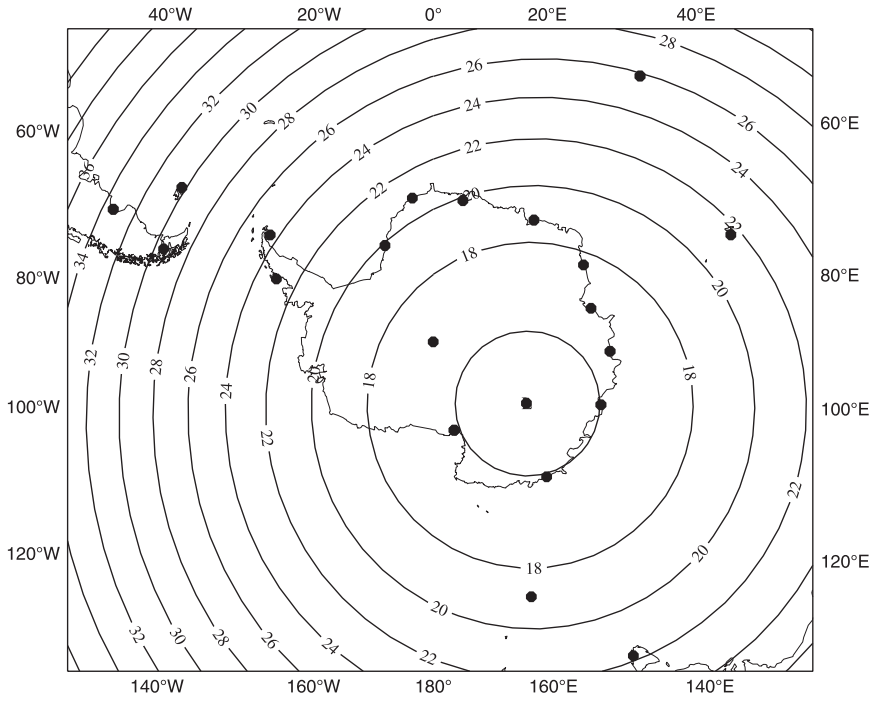

FIG. 1. Radiosoundings (black dots), regularly reported on the global telecommunication system (once to twice a day), assimilated below 50°S in the ARPEGE model. Isolines indicate the horizontal resolution of the ARPEGE model stretched over Dome C (km). Step between two isolines: 2 km.

of forecasts produced by NWP models over high latitudes is very variable. His and other studies (Adams 1997; Bromwich et al. 1999) make the assumption that the error in the forecast may come from the quality of the analysis used for the initialization of the forecast. The skill of the assimilation over these high latitudes is considerably less than over other areas (Kalnay et al. 1998).

Previous studies have put forward the low spatial and temporal density of observations at high latitudes (Barker 2005; Nordeng et al. 2007; McNally 2007; Powers 2007). The few available conventional data come mainly from radiosounding stations (black dots in Fig. 1) located in the coast of Antarctica. Inland, only the South Pole station and Dome C station (75°12′S, 123°37′E) are regularly reporting data. Because of difficulties in communication (Cullather et al. 1997), it is very hard to get information from these stations. The scarcity of conventional observations implies that each observation (e.g., radiosoundings) will have an important impact on the forecast (Leonard et al. 1997).

Since there is a lack of in situ data, the assimilation of satellite data may have a significant influence for high latitudes. Studies on GPS radio-occultation data have already shown that an increase in the number of assimilated data have a positive impact (Wee and Kuo 2004, 2008). Polar-orbiting satellites have a good coverage in space and in time over polar regions, so do the sensors onboard these platforms. However, the use of satellite radiances in data assimilation is subject to limitations. At least two main problems are standing in the way of progress: an accurate estimation of the surface temperature and surface emissivity (English 2008) and a realistic cloud detection scheme (McNally and Watts 2003). Table 1 gives a broad overview of data that are assimilated over polar regions for this study (for latitudes below 65°S). Meteorological centers assimilate various satellite observations over polar areas and sea ice. The list of channels and sensors used in the assimilation by each meteorological center depends on the characteristics of its own model, such as the altitude of the top of the model, the emissivity scheme used, etc. Details on the differences between various centers will be given later in the manuscript. This article focuses on the following sensors: the Advanced Microwave Sensor Unit (AMSU-A and AMSU-B/MHS) and the advanced infrared sounders, the Atmospheric Infrared Sounder (AIRS), and IASI.

The present study suggests different improvements to advance the state of the art in data assimilation over polar regions. The enhancements made for polar areas are listed in section 2, through the description of the model used and the modifications brought in for the

TABLE 1. Listing of the data assimilated over southern areas (latitudes below 65°S) at Météo-France over the period of our study (July 2007).

Observation type	List
Conventional (ground and airborne)	Surface data: Synop, buoy/dribu
	Airborne: AIREP
	Profiles: Pilot (for wind), radiosounding
Satellite	Microwave: AMSU-A/B, MHS radiances
	Infrared: AIRS, IASI, HIRS radiances
	Imager: MODIS (wind product)
	GPS constellation: Radio-occultation bending angles

assimilation of microwave and infrared data in the model. The consequences of these choices for satellite data assimilation over Antarctica are developed in section 3. Conclusions are presented in section 4.

2. Enhancements for polar areas

a. Model and assimilation setup

The model used in this study is the French operational global model, Action de Recherche de Petite Echelle et Grand Echelle (ARPEGE), developed in collaboration between Météo-France and the European Centre for Medium-Range Weather Forecasts (ECMWF; Courtier et al. 1994). To avoid the problem of the lateral boundary conditions in the forecast and in the assimilation (Courtier et al. 1991), ARPEGE was set up as a global model based on a stretched grid with a horizontal resolution 5 times finer over the center of interest than at the antipodes and with 60 vertical levels (0.05 hPa being the top of the model). The advantages of the stretching is to have a variable mesh with a sufficient concentration of grid points at the same time in the area of interest (associated with a lower resolution outside it) and to avoid the problem of the lateral boundary conditions associated with limited-area models (Courtier and Geleyn 1988). The ARPEGE model uses an advanced four-dimensional variational data assimilation (4D-Var) assimilation system (Rabier et al. 2000) and a wide range of conventional and satellite observations. In the assimilation, an adaptative variational bias correction method is applied for the treatment of the radiance biases to reduce biases between satellite observations and their model equivalent (Auligne et al. 2007). One can also mention that during the assimilation, the minimization, and thus the calculation of the analysis increment (the difference between the analysis and the background of the model), is done using a regular nonstretched grid. Moreover, it is important to mention how the statistics of the forecast errors are estimated in this system (the background error covariance matrix). An ensemble assimilation is used to calculate the background error covariance matrix (Belo Pereira and Berre 2006). This ensemble is composed of six perturbed global members coming from a nonstretched model. It is then not deemed necessary to change this background error matrix computation when changing the stretching of the model.

The horizontal resolution of the model has an impact on the forecast accuracy. For example, a poor horizontal resolution can induce a bad representation of the orography for the Antarctic Peninsula and consequently a bad representation of mesoscale systems. In operations, at Météo-France, the ARPEGE grid is centered over Europe; thus, it follows that the orography may not be well represented over Antarctica. In this study, a new geometry was used to get a good resolution over Antarctica. The center has been moved southward, from Europe to the Dome C Station. With this stretched grid, the horizontal scale is less than 20 km over Antarctica (circles in Fig. 1), with a resolution less than 30 km for latitudes below 60°S.

The impact of the new geometry on the representation of the orography in the model is illustrated in Fig. 2. The orography before the modification is shown on the left-hand side and on the right-hand side, after the modification. The representation of the orography in the model is more precise over Antarctica with the new center, with the disappearance of some unphysical features on the old version due to the spectral representation. As illustrated in both maps, the orography of Antarctica has some asymmetric features: in the western part of the continent (mainly comprising the peninsula) the maximum orography is about 1 km in contrast with the high orography of the eastern part where mountains reach 4 km high.

More detailed tests have been performed to quantify the impact of this modification. Figure 3 shows some statistics calculated over 10 days in September 2007, using outputs of the model with the initial geometry (center in France—solid line) and with the new geometry (center in Antarctica—dashed line). The number of observations (radiosoundings located at latitudes below 60°S) for each layer of 50 hPa is presented on the right-hand side. This same figure shows, with the new geometry and for all altitudes, the increase of data assimilated in the model for Antarctica. On the left-hand side, is plotted the root-mean-square (rms) of the difference between the observations (radiosoundings) and the background for the temperature. A decrease of the root-mean-square can be noted for all altitudes. This means that, for this area and with the new geometry, the model is closer to the observations than it was with the old geometry. There is a noticeable increase in the number of observations

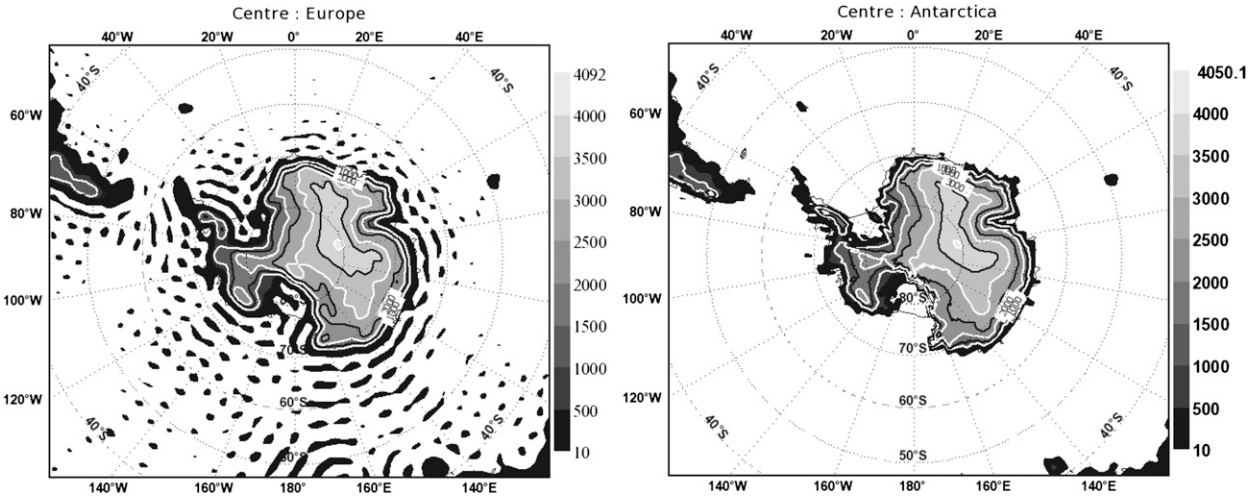

FIG. 2. Representation of model orography over Antarctica with the center of the model (left) in France and (right) at Dome C. Isolines are each 500 m.

above 100 hPa for both experiments. This change in the slope of the profile comes from the use of 50-hPa layers in the calculation and the presence of an important number of observations with pressure between 0 and 50 hPa because it represents a deep atmospheric layer. In terms of forecast accuracy, statistics, for tuned and operational models, have been calculated over the same period for thermodynamical and dynamical variables, using radiosoundings as a reference. A positive impact is present mainly for altitudes below 50 hPa for all forecast ranges (from 0 to 96 h) for the Southern Hemisphere area and more precisely over Antarctica. An rms improvement of 2 m (up to 6 m) in geopotential, of 0.1 K in temperature, and 0.3 m s^{-1} in wind speed are found below 100 hPa at all forecast steps.

This modification of the model geometry improves the representation of the orography in the model over Antarctica and will help ameliorate data assimilation. More in-depth studies on the use of satellite data in the assimilation were also carried out.

In particular, improvements in the representation of surface emissivity and temperature are necessary to decrease the number of observations rejected during the assimilation system. In the following, studies toward a better estimation of surface emissivity at microwave frequencies will be presented as well as feasibility studies undertaken to assimilate as many relevant infrared and microwave observations as possible over Antarctica.

b. Microwave observations

Satellite instruments measure the top-of-the-atmosphere radiances at given frequencies. These radiances are related to geophysical parameters (e.g., temperature and humidity profiles) by the radiative transfer equations, parameterized by a Radiative Transfer Model (RTM). Other parameters are needed as inputs to the RTM model such as surface parameters to characterize the radiation emitted by the surface. For satellite data assimilation, the RTM provides the link between the atmospheric state and the observations, through the observation operator. For ARPEGE, the RTM is the Radiative Transfer for the Television and Infrared Observation Satellite (TIROS) Operational Vertical Sounder (RTTOV) fast radiative transfer model (Eyre 1991; Saunders et al. 1999; Matricardi et al. 2004). RTTOV simulations need to be accurate enough to assimilate satellite observations. This condition is usually not satisfied if the surface temperature and/or emissivity are not well described. In the assimilation, the surface temperature is usually provided by a short-range forecast from an analyzed surface temperature using synoptic observations. Because of the scarcity of observations over Antarctica, surface temperature may be far from accurate. Trigo and Viterbo (2003) have shown that errors about this parameter can restrict the assimilation of observations from polar-orbiting sounders. Similarly with the surface temperature, the estimation of the surface emissivity is very complex. Accurate models exist to estimate the surface emissivity over sea (Hewison and English 2000; Deblonde and English 2000). Over land, sea ice and mainly cold surfaces, the variability of the surface emissivity involves complex mechanisms (Weng and Yan 2003; King and Turner 1997; Comiso 2000). For a proper modeling of cold surface emissivity, one should take into account the vertical structure of the surface (presence of

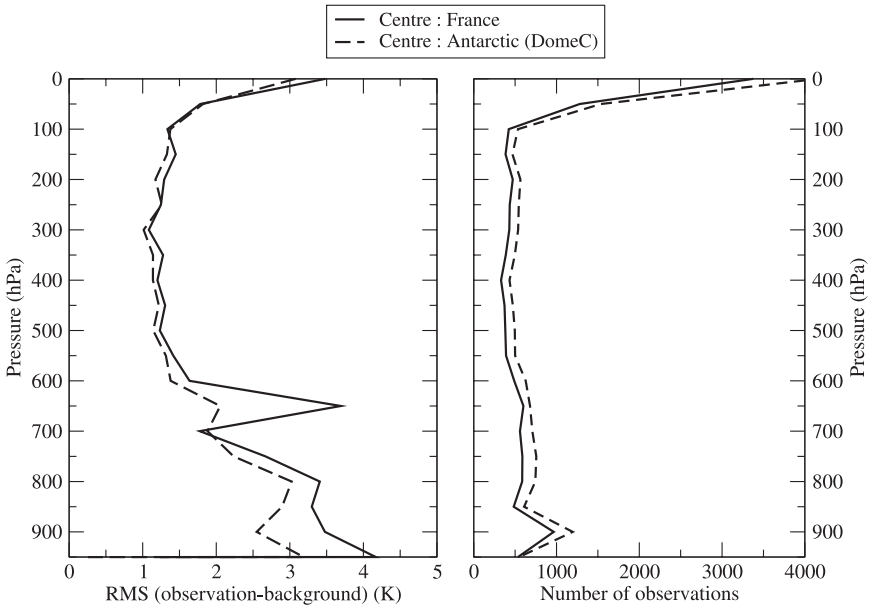

FIG. 3. Impact on the change of geometry by comparison of an experiment with the model center in France (solid line) and the second one with the model center in Antarctica (dashed line). (left) The rms of the difference between observations (radiosounding located below latitude 60°S) and background for the temperature (K) has been plotted. (right) The number of observations assimilated. Statistics in 50-hPa layer have been calculated over a 10-day period.

snow, first-year ice, multiyear ice) and should have a good knowledge of the physical properties of the different layers. Interactions between microwave radiation and the cold surface also have to be accounted for, since they vary as a function of the frequency (variation of penetration depth; English 1999; Mathew 2007; Picard et al. 2007). However, for data assimilation, a compromise that will meet NWP requirements has to be found between the cost and the ability of a model to accurately describe the surface emissivity. In the present work, developments have been directed toward a better modeling of the surface emissivity over Antarctica but more efforts should be made toward a more accurate estimation of the surface temperature. This point will be further examined in an upcoming work.

1) EMISSIVITY CALCULATION

The present work relies on a method, fully described in (Karbou et al. 2006), hereafter the ''dynamical approach.'' This approach is based on the direct estimation of the land surface emissivity using satellite observations from selected window channels. The dynamical approach is interfaced with the RTTOV model. First, the emissivity is calculated using brightness temperatures from well-selected window channels. Second, the retrieved emissivity from the closest window channel to sounding channels (in frequency) is used to simulate brightness temperatures (hereafter ''Bts'') of other AMSU sounding channels. Emissivities from AMSU-A channel 3 (50.3 GHz) and AMSU-B channel 1 (89 GHz) are assigned to AMSU-A temperature and AMSU-B humidity sounding channels, respectively. The dynamical approach has been found very helpful to increase the correlations between observations and simulations of AMSU-A and AMSU-B sounding channels and to assimilate more observations over land. This approach has been implemented in the ARPEGE operational system since July 2008.

Over sea ice, the ARPEGE operational system uses a simplified version of Grody (1988) emissivity model for AMSU-A and a constant value of 0.99 for AMSU-B. To improve the assimilation of AMSU data over sea ice, the emissivity dynamical approach'' initially developed for land surfaces has been extended to estimate emissivities over sea ice. Using this method, sea ice and Antarctica emissivities have been retrieved for two 1-month periods (July 2007 and January 2008) using observations from AMSU window channels (23.8, 31.4, 50.3, 89, and 150 GHz). Figure 4 shows the emissivity variation with frequency and with season over sea ice using the dynamical approach. Regardless of frequency, the July emissivities are systematically higher than the January ones. This is consistent with the fact that during the austral winter, sea ice covers a large area and the amount

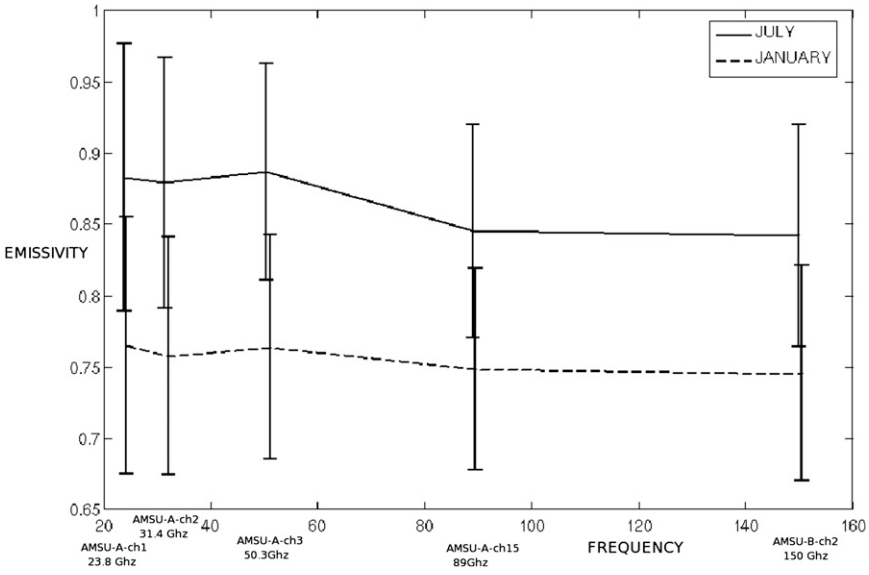

FIG. 4. Mean emissivity over sea ice, as a function of the frequency (unit: GHz, on *x* axis) for two months: July 2007 (solid line) and January 2008 (dashed line). Vertical bars indicate the standard deviation associated with the mean emissivity for each frequency.

of first year ice is more important than during summer. In January, the sea ice melts and mixes with open water and consequently the mean emissivity is smaller. The emissivity slightly decreases with increasing frequencies. This is consistent with Mathew's findings over sea ice (Mathew 2007). Figure 5 shows mean emissivity maps derived from January and July observations of AMSU-B channel 1 (89 GHz) over sea ice and over Antarctica (at the top) and the same maps from AMSU-A channel 3 (50 GHz) (at the bottom) using the dynamical approach. As expected, the emissivity maps exhibit some variability in space and in time. Over land, emissivities vary from 0.65 (the eastern part of the continent) to 0.85 (the peninsula and the coast). Over sea ice, the emissivity fluctuates from January (summer) to July (austral winter). During July, sea ice emissivity can reach 0.95. Ideally, sea ice surface emissivities should be compared to some independent emissivity measurements. As we are not able to perform such a comparison, retrieved emissivities and emissivities coming from the operational system are further evaluated by comparing observed and simulated Bts at some AMSU sounding channels.

Emissivity from AMSU-A channel 3 and from AMSU-B channel 1 (89 GHz) are used to simulate Bts, for example, at AMSU-A channel 4 (52.8) and channel 5 (53.596 $\pm$ 0.115 GHz) and at AMSU-B channel 2 (150 GHz) and channel 3 (183 GHz), respectively. RTTOV model provides Bts simulations and uses as input information from short-range forecasts (6-h forecasts). The differences between observations and simulations (hereafter noted departures) are computed for AMSU-A and AMSU-B channels using the first 20 days of July 2007. The departures obtained when emissivities from the operational system are used, are noted DEP-CONTROL whereas those obtained when the emissivity from the dynamical approach are used are noted DEP-EXP. One should bear in mind that AMSU-A channel 4 and AMSU-B channel 2 are very important for the assimilation of AMSU measurements since they are used in quality control tests to discriminate between observations that the assimilation system is able to model and thus to assimilate, and between other observations rejected by the system. Smaller departures for these channels imply the possibility to assimilate more satellite data. Histograms for AMSU-A channel 5 and AMSU-B channel 3 bring information on the impact for assimilated channels. The details of assimilated channels for AMSU-A/B are described in section 2b(2).

DEP-CONTROL (dashed curves) and DEP-EXP (solid curves) departures, over sea ice, are compared in Fig. 6. For AMSU-A test channel (Fig. 6, top-left-hand panel), the DEP-EXP histogram is thinner and more centered around zero than the DEP-CONTROL histogram. This means that the performances of the RTTOV model are improved when the emissivity is described using the dynamical approach. For AMSU-B test channel (Fig. 6, top-right-hand panel), the DEP-CONTROL histogram shows a mean bias of about -25 K (due to the use of a constant emissivity value in operations) whereas this bias is largely reduced in the DEP-EXP histogram. However,

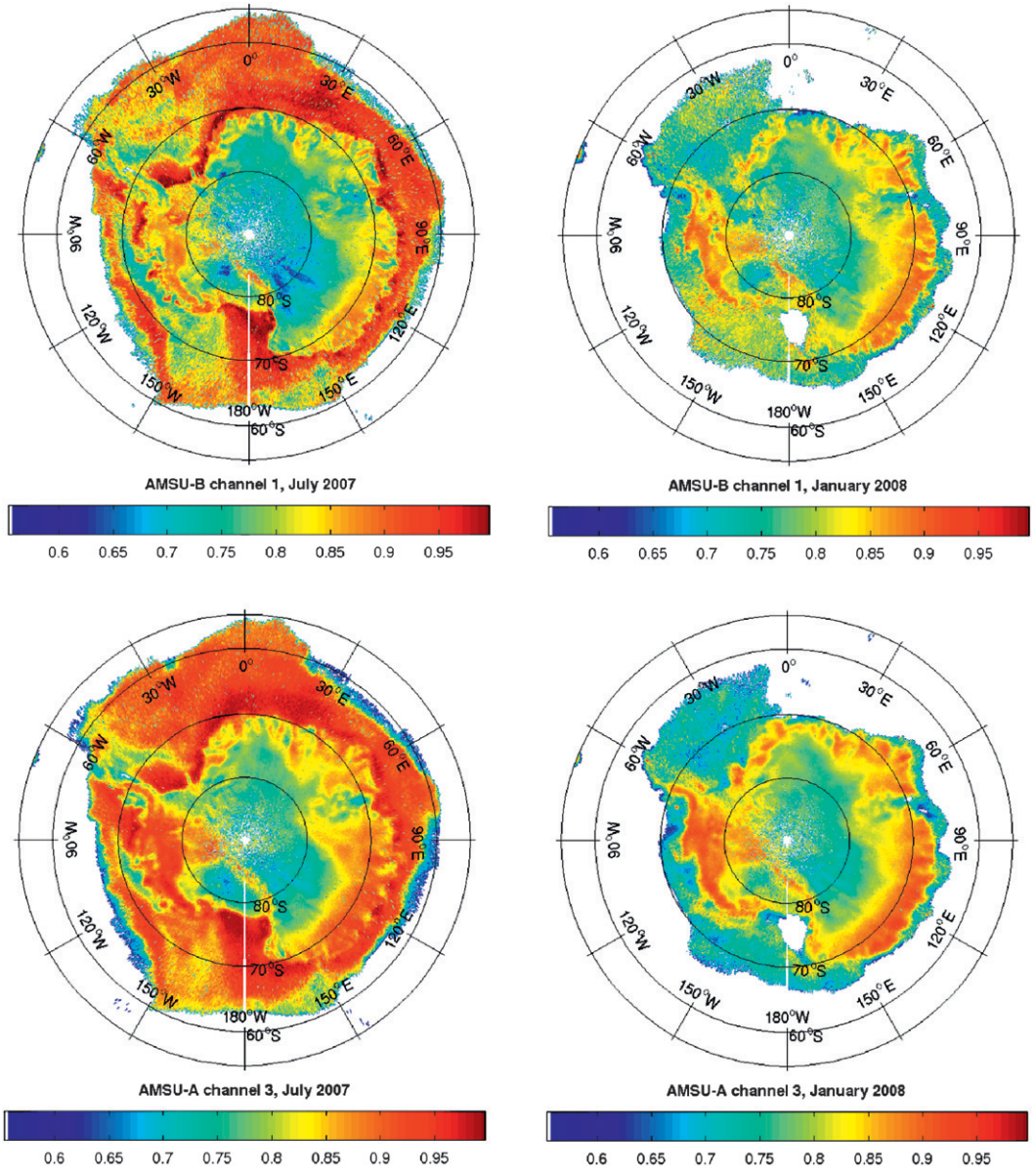

FIG. 5. (top) Mean emissivity for channel 1 (89 GHz) of AMSU-B in (left) July 2007 and (right) January 2008 over sea ice and land. (bottom) Mean emissivity for channel 3 (50 GHz) of AMSU-A in (left) July 2007 and (right) January 2008 over sea ice and land. All emissivities have been derived using the dynamical approach.

although significantly better than the control one, the DEP-EXP histogram still indicates a bias. As mentioned before, the retrieved emissivity from channel 1 (89 GHz) is assigned to AMSU-B sounding channels without any frequency parameterization. The variation of sea ice emissivity with frequency is not negligible as illustrated in Fig. 4. It may appear more convenient to estimate emissivity at AMSU-A channel 4 and at AMSU-B channel 2 instead of using window channels for that estimation. However, this alternative cannot be adopted because 1) AMSU-A channel 4 and AMSU-B channel 2 are used in the assimilation as quality control (QC) test channels and 2) the emissivity, if computed at sounding channels, would be very noisy due to weaker atmospheric transmission. The bias in DEP-EXP for AMSU-B channel 2 can be corrected if an adequate frequency parameterization is applied to account for the emissivity variation when the frequency rises from 89 to 150 GHz. A linear frequency parameterization has been adopted: it consists in determining the mean bias between the

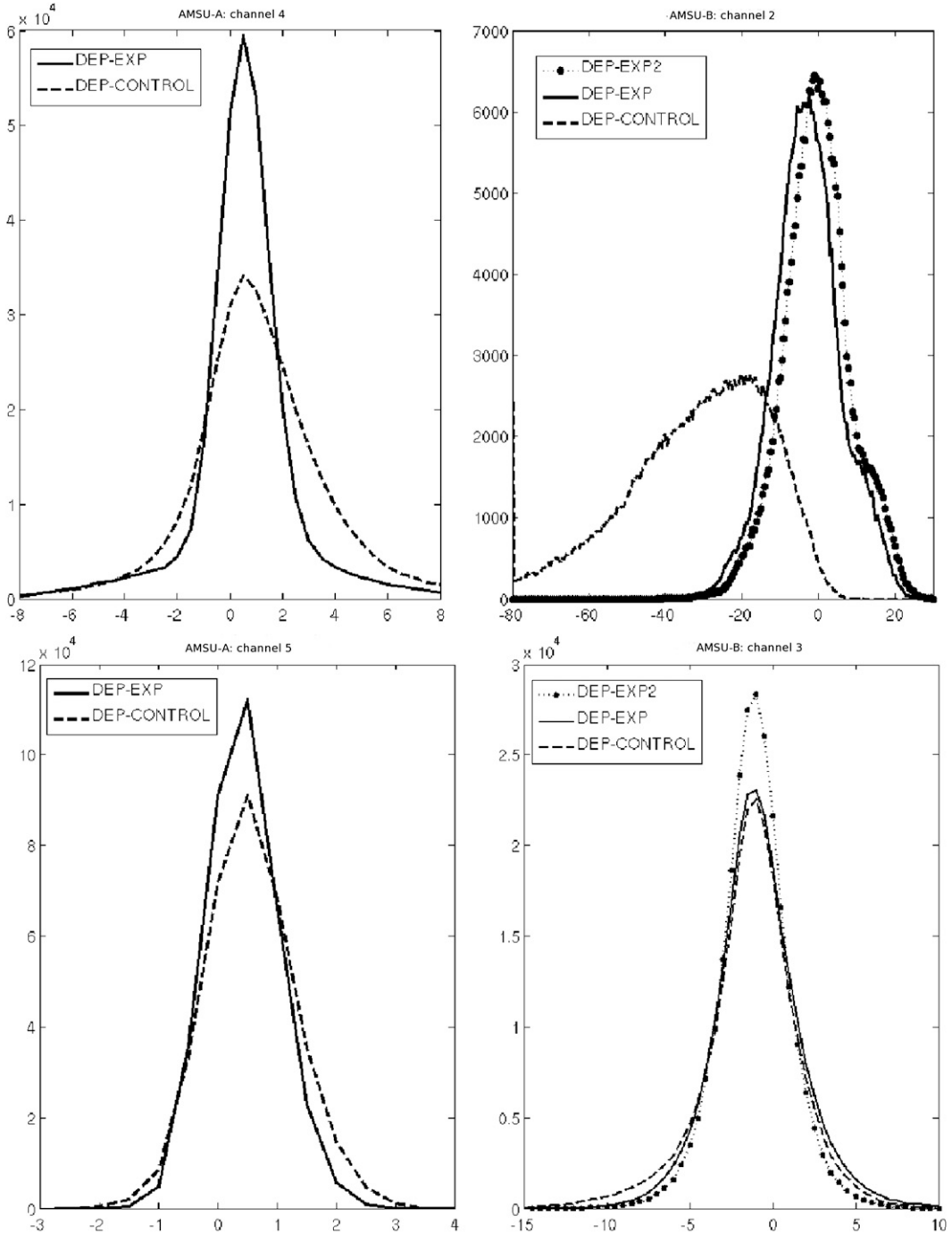

FIG. 6. Histograms of the innovation for (top left) AMSU-A channel 4 and (top right) AMSU-B channel 2 over sea ice in July 2007. Same histogram for (bottom left) AMSU-A channel 5 and (bottom right) AMSU-B channel 3. CONTROL is using Grody's scheme for the calculation of AMSU-A emissivity and a constant value for AMSU-B. EXP uses the dynamical approach for both sensors. EXP DYN is the dynamical approach classic, without bias addition for AMSU-B.

emissivity at 89 GHz and the emissivity at 150 GHz during July 2007. Emissivity biases have been computed over sea ice and over Antarctica and have been used to correct the estimated emissivity at 89 GHz. The emissivity changes are $\Delta\epsilon = -0.016$ for sea ice and $\Delta\epsilon = 0.00484$ for Antarctica. Departures at AMSU-B channel 2 have been calculated using corrected 89-GHz emissivities (hereafter DEP-EXP2). Figure 6 shows

TABLE 2. List of the criteria for AMSU-A channel assimilation at Météo-France. The letter "C" stands for CONTROL and the comments in italic are for the operational model. The letter "E" stands for EXP and the comment in roman font are for the framework of the IPY.

Criteria	1	2	3	4	5	6	7	8	9	10	11	12	13	14	15
$3 <$ scan position < 28					E/C	E/C	E/C	E/C	E/C	E/C	E/C	E/C	E/C		
Land							E/C	E/C	E/C	E/C	E/C	E/C	E/C		
Alt < 1.5 km					E										
Alt < 500 m					C										
Alt < 2 km						E									
Alt < 1.5 km						C									
Sea ice					E	E	E/C	E/C	E/C	E/C	E/C	E/C	E/C		
Open sea					E/C	E/C	E/C	E/C	E/C	E/C	E/C	E/C	E/C		
Clear					E/C	E/C	E/C	E/C	E/C	E/C	E/C	E/C	E/C		
$\lvert obs - background\rvert_{ch4} > 0.7$ K [and $CLWP(ch1, 2) < 0.1$ kg m^2 over sea]															
Cloudy								E/C	E/C	E/C	E/C	E/C	E/C		
$\lvert obs - background\rvert_{ch4} > 0.7$ K [and $CLWP(ch1, 2) > 0.1$ kg m^2 over sea]															

DEP-EXP2 histograms over sea ice (dotted curve with points). The bias in DEP-EXP2 has been reduced by about 3 K compared with DEP-EXP. The latter configuration has been adopted to improve the assimilation of AMSU measurements over Antarctica and the surrounding sea ice.

In the lower part of Fig. 6, are represented additional plots for assimilated channels: channel 5 of AMSU-A (left-hand panel) and channel 3 of AMSU-B (right-hand panel). In these figures, one can note that the improvement of the emissivity calculation also has a positive impact on simulated brightness temperature. Both histograms (DEP-CONTROL and DEP-EXP) for these assimilated channels are also thinner and centered near the zero line. To conclude, departures for the QC test channels were improved, which meant an increase in the number of data that can be assimilated. In parallel, a direct impact of the emissivity change was noticed for the remaining sounding channels. The selection criteria for AMSU-A/-B data have also been modified (see next section). Assimilation experiments will be presented in section 3.

2) ON THE CRITERIA OF SELECTION OF AMSU OBSERVATIONS

In addition to the modification of the surface emissivity, the criteria for the assimilation of AMSU-A/B have been changed for high latitudes. In operation, the selection of assimilated channels is based on surface types, scan position, cloudiness, orography, and departures in the QC test channels. This selection is quite conservative and needs to be slightly relaxed. In other meteorological centers, channels are also assimilated according to various criteria. Channel 14 of AMSU-A is assimilated in many centers, but is not in the Météo-France operational system because this assimilation should be compatible with the top of the model. For the remaining AMSU-A channels, the assimilation is very similar, except for the thresholds on the orography. Moreover, only few centers assimilate AMSU-B data over sea ice and Antarctica but with many restrictions. In the assimilation experiments, some of the criteria of the data selection were indeed modified in order to use more observations. Tables 2 and 3 summarize the list of the assimilated channels in the experiment versus the operational model at Météo-France, for high latitudes for AMSU-A and AMSU-B, respectively. Before going into details in the change of criteria between our experiment and the operational model, it is important to recall that no channels are very sensitive to the surface (i.e., channels 1–4, for AMSU-A and channels 1 and 2, for AMSU-B) are assimilated because of still remaining uncertainties about the surface emissivity and the surface temperature. For

TABLE 3. As in Table 2, but for AMSU-B channels.

Criteria of use	1	2	3	4	5
$9 <$ scan position < 82			E/C	E/C	E/C
Land					
Alt < 1.5 km				E	E
Alt < 1 km				C	
Alt < 3 km			E		
Alt < 1.5 km			C		
Land, sea ice, open sea (E)			E/C	E/C	E/C
$\lvert obs - background\rvert_{ch2} < 5$ K					
Land, open sea (C)			E/C	E/C	E/C
$\lvert obs - background\rvert_{ch2} < 5$ K					
$Ts > 278$ K					

AMSU-A, the main difference, with the operational configuration, consists in the assimilation of channels 5 and 6 over sea ice. For AMSU-B, in operations, no data are yet assimilated over polar area, mainly because of a test on the surface temperature (at 278 K). Removing the threshold, in addition to the modification of the emissivity calculation, makes it possible to assimilate channels 3, 4, and 5 over sea ice and Antarctica. The relevance of the thresholds on orography has been investigated for both AMSU-A/B. These thresholds are used to prevent a too large contribution of the surface for the various channels. A better modeling of emissivity allows a moderate increase of the orography thresholds and consequently an increase in the number of assimilated observations. For example, the orography threshold for AMSU-A channel 5 has been increased from 0.5 to 1.5 km. The orography threshold changes are expected to have a nonnegligible impact over quite a broad coastline around Antarctica (see the orography map of Antarctica in Fig. 3).

To examine the impact of these modifications on microwave emissivity calculation (emissivity scheme and modification of thresholds), the number of assimilated observations, the mean and the rms of associated departures were calculated for AMSU-A/B over the first 20 days of July 2007 for assimilated observations. Results, given after bias correction, are presented in Fig. 7 by surface types: land (Antarctica), on the right-hand side and sea ice on the left-hand side. The six top plots show results for AMSU-A and the six bottom ones are for AMSU-B. For all plots, the channel number is on the x axis. Some differences appear between DEP-CONTROL and DEP-EXP for all AMSU-A assimilated channels and for both surfaces. Over sea ice, the rms of the new assimilated channels (5 and 6) has the same magnitude as the others (from 7 to 11) between 0.2 and 0.3 K. Moreover, the plots show an increase in the number of data assimilated for each channel over sea ice with DEP-EXP experiment. Over land, the variation of the number of data is weaker and depends on channels. In terms of means, the magnitude decreases when moving from DEP-CONTROL to DEP-EXP experiments. For AMSU-B, in DEP-CONTROL, no data are assimilated over sea ice and almost none over land because of a threshold on the surface temperature. The departure rms of the data assimilated is between 2 and 3 K over sea ice. Over land, the departure rms is around 3 K. For AMSU-A, mean biases are between −0.2 and 0.6 K over sea ice and around 1 K over land. It can be noticed, that in these experiments, the observation error statistics are those presented in Table 1 of Karbou et al. (2010). The effect of all these changes from an assimilation point of view will be further examined in section 3.

c. *Infrared observations*

This study also focuses on AIRS and IASI infrared sensors. These high spectral resolution sensors are able to provide unprecedented information on the atmospheric temperature and composition at a higher vertical resolution than filter infrared radiometers can achieve (McNally 2007). IASI data have been available since the beginning of 2007, and have gradually started to be assimilated in models. Since IASI provides rather innovative observations, the first assimilation implementations have been intentionally quite conservative. Currently, in most NWP centers, IASI observations are not assimilated over sea ice nor over land. In the Météo-France operational system, only channels with a wavenumber between 651.05 and 721.54 cm^{-1} are used for AIRS and between 672.0 and 751.25 cm^{-1} for IASI, respectively. At the time of this study, only data over sea were operationally assimilated (which is no longer the case).

Clouds have an important radiative impact on infrared radiances. As assimilated radiances are mostly associated with clear-sky conditions, further simulations in cloudy-sky conditions are not only necessary but badly needed in NWP. An effective cloud detection scheme is, however, necessary to eliminate data contaminated by clouds (McNally 2007). The Antarctic coast is known to be among the cloudiest places on the earth, with a mean total cloud cover of about 80% (Turner and Pendlebury 2004). King and Turner (1997) have studied this cloud distribution. Stratiform clouds are the most frequent ones (stratus, nimbostratus, altostratus, and cirrus), but some cumulonimbus can also develop. Inland, because of the high orography, low to midlevel clouds are scarce, whereas thinner high clouds prevail. Visual observation of clouds over Antarctica is difficult because of meteorological conditions (e.g., blowing snow) and the lack of luminosity in winter (King and Turner 1997). King and Turner (1997, p. 104) have noticed a disagreement between the International Satellite Cloud Climatology Project (ISCCP) cloud cover and conventional observations, mainly for thin ice clouds at high altitudes [i.e., polar stratospheric clouds (PSCs)].

The identification of clouds over Antarctica is a rather difficult issue in data assimilation. Some cloud detection schemes are based on the comparison with the surface temperature (Goldberg et al. 2003). But in polar areas, the cloud temperature is either similar to or warmer than the surface temperature, which can make these schemes inefficient. Other cloud detection schemes rely on model simulated radiances. However, these simulated radiances can be of poor quality in these areas because of the general performance of models. Therefore, an evaluation of the cloud detection scheme, used in the

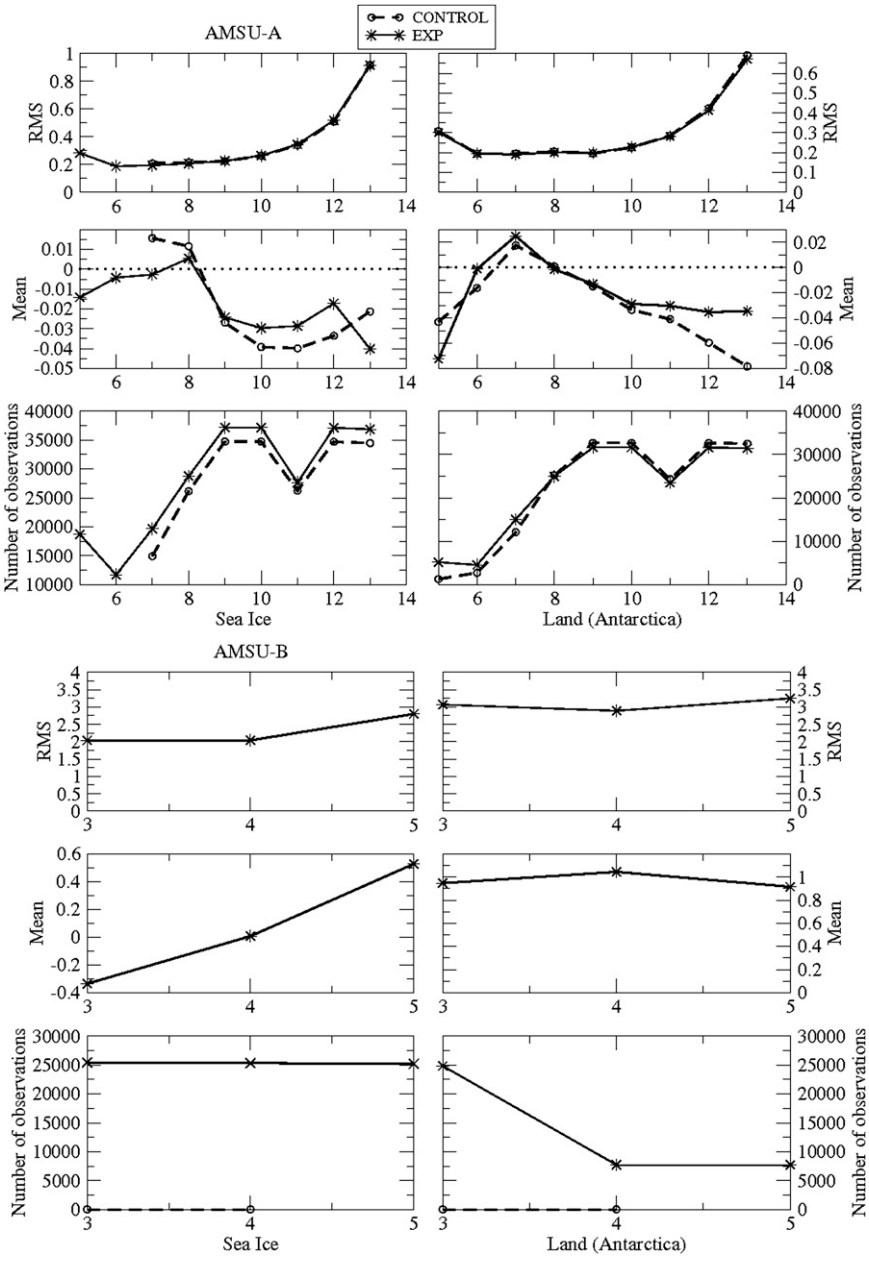

FIG. 7. Difference between CONTROL (dashed line with circles) and EXP (solid line with stars) for the assimilated observations (right) over land and (left) over sea ice. (top) The rms plot, (middle) mean plot, and (bottom) the number of observations are plotted. The computations were performed over the first 20 days in July 2007 for latitudes below 55°S. Results have been calculated after bias correction. Channel numbers for both AMSU-A/B are indicated on the *x* axis in all figures.

assimilation system, is necessary and is a prerequisite before extending the usage of data. This study uses the ECMWF scheme for its cloud detection (McNally and Watts 2003). Its aim is to detect clear channels within a measured spectrum rather than to locate totally clear pixels. Some studies have already evaluated this cloud detection method, among them (Dahoui et al. 2005) and (Pangaud et al. 2009).

An example of the skill of the cloud detection method is presented in the following. Two parameters are compared in Figs. 8 and 9. The first one is the cloud-top pressure from the Moderate Resolution Imaging

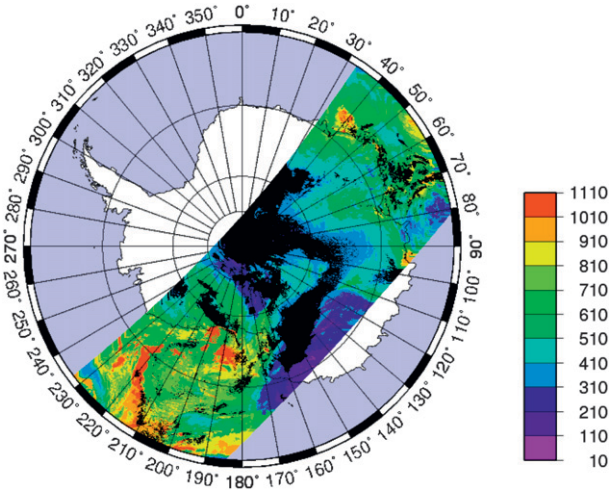

FIG. 8. Cloud-top pressure product from MODIS on *Aqua* between 1020 and 1050 UTC 1 Aug 2007. Pressure from 10 to 1000 hPa every 10 hPa. Black areas are associated with no clouds. Lines indicate the latitude and longitude every 10°.

Spectroradiometer (MODIS) sensor on the *Aqua* satellite (product MYD06_L2), which is considered as a reference (Fig. 8). The second one is the indicator of cloud effect on the radiance, estimated from the cloud detection method (Fig. 9) for the AIRS swath (at the top) and the IASI swath (at the bottom), for two channels peaking at different heights. The figures correspond to a part of the MODIS swath between 1020 and 1050 UTC 1 August 2007.

Because of differences in orbit between *Aqua* and MetOp, outputs can only be compared in the southwestern part for the IASI sensor. In Fig. 10, typical weighting functions are shown for the two sensors IASI and AIRS at channels used in Fig. 9. The maximum of the weighting function for IASI channel at 686.50 cm^{-1} (721.25 cm^{-1}) is 85 hPa (287 hPa). Consequently, the channel at 686.50 cm^{-1} is sensitive to high clouds and the channel at 721.25 cm^{-1} is sensitive to the presence of high and medium clouds. The channel at 721.25 cm^{-1} is the lowest channel assimilated over sea ice and land. In Fig. 9, for the channel at 686.50 cm^{-1}, few pixels are found cloudy in our area of interest, an area encompassed within 60° and 85°S and within 230° and 160°E. In Fig. 8, for this same area, MODIS detects clouds with cloud-top pressure reaching 100 hPa. In Fig. 9, the channel at 721.25 cm^{-1} shows a more widespread area of clouds that is in agreement with the presence of lower clouds in the collocated area. The same comments can be made for the indicator of cloud effect along the AIRS swath. Selected channels have a similar maximum of weighting function as IASI channels, as described before. For the channel at 673.64 cm^{-1} peaking near 85 hPa, very few pixels have been detected cloudy. But when compared to the magnitude of the cloud-top pressure of MODIS, few clouds have a high pressure (purple and dark blue color). The method misses a few clouds but is in agreement with results obtained with the IASI swath. The same conclusions can be found with the channel at 702.74 cm^{-1}. In conclusion, the cloud detection method seems to give quite good results over this area for this swath and for other examined cases. More in-depth studies are however necessary to improve the cloud detection scheme. In this study, the cloud detection scheme has been used unchanged.

To assimilate more IASI and AIRS channels over land and over sea ice, it had been necessary to make many changes in the data selection, as it had been done with microwave observations. For AIRS, in addition to the 54 channels over open sea already assimilated, a further 22 channels over sea ice and 51 over land have been added. For IASI, 32 channels over sea ice, 50 channels over land, and 14 additional channels (e.g., 64 channels) over open sea have been selected for assimilation. It should be recalled that, at the time of this study, data over sea only were assimilated for AIRS and IASI sensors. Moreover, some differences can be noted between the number of channels over land and over sea ice for both sensors. Channel selections are based on statistics on the difference of observation (brightness temperature) and background before monitoring, on the one hand and on the other hand on the shape of the weighting function. The sea ice channel selection is a subgroup of the land channel selection. Statistics over sea ice are more difficult because of the fluctuating seasonal cover of ice, which leads to a smaller number of channels that can be selected over sea ice.

In Fig. 11, a summary of IASI (on the left-hand side) and AIRS (on the right-hand side) channels assimilated as a function of their wavenumber have been plotted for different surface types. A black dot indicates that a channel is assimilated in EXP only and a gray one that it is assimilated in CONTROL and EXP experiments. To choose which IASI channels can be assimilated over sea ice and over land, radiative transfer simulations have been run and the corresponding departure characteristics have been examined for clear channels. Figure 12 shows the average and the rms of departures (after bias correction) for three surface types (land, sea ice, and open sea) as a function of the wavenumber, for latitudes below 50°S, and only for channels not affected by clouds. Subplots on the lower figure indicate the number of observations as a function of the wavenumber. Higher channel numbers are more sensitive to the lower atmosphere, and thus more affected by clouds, therefore the number of clear pixels decreases as the channel number

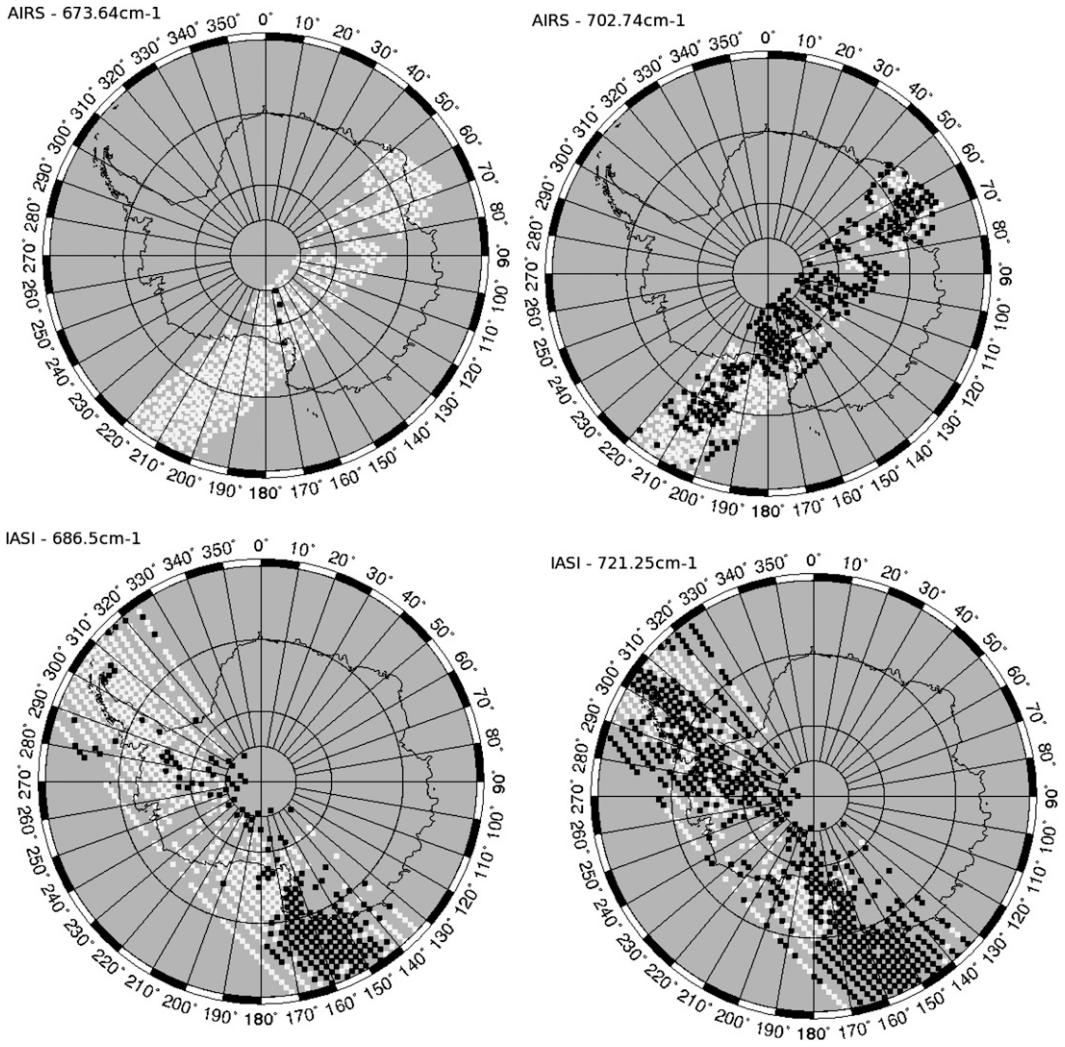

FIG. 9. Cloud output from the cloud detect method along the AIRS swath on the top and along the IASI swath on the bottom between 1020 and 1050 UTC 1 Aug 2007. AIRS channels are (left) 673.64 and (right) 702.74 cm^{-1}. IASI channels are (left) 686.5 and (right) 721.25 cm^{-1}. Black (white) pixel means that the channel is cloudy (clear) for this pixel. Lines indicate the latitude and longitude every 10°.

increases. For channels ranging from 672 and 721.55 cm^{-1}, the rms is close to 0.2 K. Beyond the channel at 721.55 cm^{-1}, the rms increases for both land and sea ice surfaces. Such a change feature is also noticeable for the average plot (in the middle, Fig. 12). A peak in the number of observations for channel at 719.50 cm^{-1} can be noticed. It can be explained by the shape of the weighting function profile for this channel (the peak is higher in the atmosphere than for neighboring channels, similar to channels below the wavenumber 700 cm^{-1}). Consequently, the channel with the wavenumber of 721.55 cm^{-1} was chosen to be the lowest candidate for the assimilation of IASI over sea ice and over land. The same procedure has been applied to AIRS channels (Fig. 13). In this figure, it is easy to see that beyond the wavenumber of 722 cm^{-1}, the rms and the bias increase for all surface types. For both sensors, the number of observations over land is smaller than for over sea ice because statistics have been calculated only with observations accepted by the system (after rejection by the cloud detection and other quality control tests).

3. Assimilation experiments

a. Diagnostics on additional data

In a first step, assimilation experiments have been run to study the relative impact of additional data from

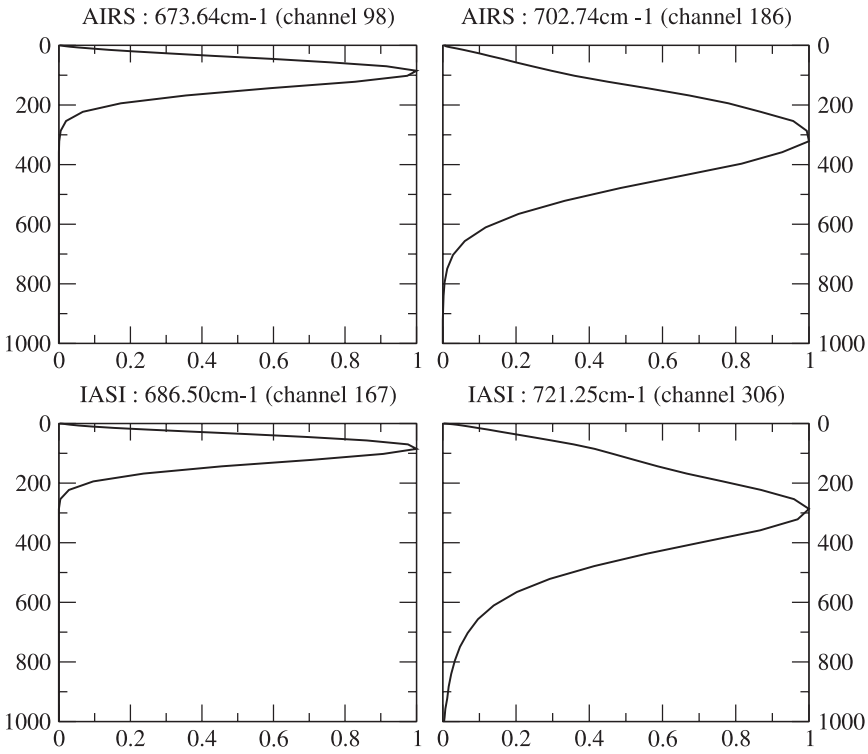

FIG. 10. Weighting functions for (top) AIRS channels are 673.64 and 702.74 cm^{-1} and (bottom) IASI channels 686.5 and 721.25 cm^{-1}. The *y* axis is the altitude (hPa).

either microwave or infrared sensors using configurations presented in the previous sections. These experiments reveal that assimilating many more infrared or microwave observations over Antarctica and sea ice is beneficial for our assimilation system. In a second step and to benefit from the information content of both infrared and microwave observations, another experiment, called EXP, has then been run. In EXP both additional infrared and microwave data are assimilated. This experiment is compared with a control experiment, called CONTROL, which is representative of the operational system, at the date of this study, and which does not assimilate any other additional data. All experiments used the Antarctica tuned model (Fig. 1). The assimilation period lasted from 15 July to 5 August 2007. The first 6 days of the run have been discarded to allow an optimal setup of the experiments, excluding a warming-up phase in our diagnostics. Unless otherwise specified, all comparisons and diagnostics are made using these run outputs. The July–August period corresponds to the first austral winter season during which IASI data have been available. During this season, the sea ice extent is sufficiently large to make the impact of the additional data assimilation over the three surfaces more relevant. Examples of the increase in the number of the assimilated data have been presented in a previous section in Fig. 7 for AMSU-A/-B sensors and in Fig. 11 for AIRS and IASI sensors.

To conclude on the datasets used in both experiments, the evolution of the number of observations has been estimated for both experiments (EXP and CONTROL), for south polar areas (latitudes below 65°S). Ten bars are drawn in Fig. 14 associated, respectively, with the following data, surface observations (Synop), atmospheric motion vectors (SATOB), drifting buoys (Dribu), radiosoundings (RS), GPS radio-occultations (GPS), and radiances from the following instruments: the High Resolution Infrared Radiation Sounder (HIRS), AMSU-A, AMSU-B/MHS, AIRS, and IASI. The increase in assimilated data, in experiment EXP, is confirmed in this figure. For experiment EXP, the vast majority of observations assimilated over this area comes from satellite data, both infrared (AIRS, IASI) and microwave (AMSU-A and AMSU-B); whereas, for experiment CONTROL, the majority of data comes from other satellite data, the AMSU-A sensor, followed by the SATOB and the GPS radio-occultation data, respectively. Ground and airborne data are a minority in both cases.

The next section will document further the changes brought by EXP, comparing the model background with respect to other observations and showing the impact on the forecast.

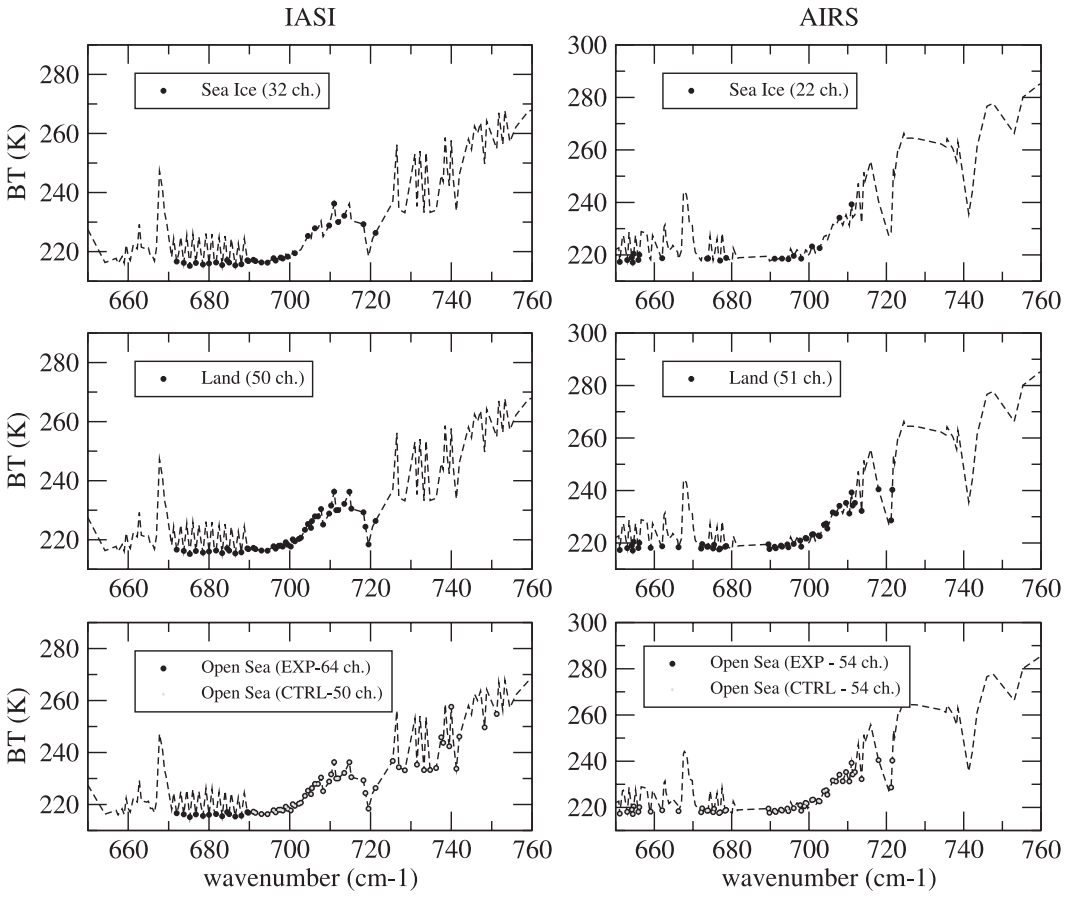

FIG. 11. Indicators of the channels assimilated for (left) IASI and (right) AIRS as a function of the three surface types: sea ice, land, and open sea. A typical brightness temperature spectrum, on 24 Jul 2007, has been plotted as a dashed line as a function of the wavenumber. For each surface type and sensor, a black dot indicates that the channel is assimilated in EXP, a gray one indicates that the channel is assimilated in CONTROL and EXP.

b. Estimation of the impact

The impact of the assimilation of the data listed in section 2 will be presented with various diagnostics.

1) THE MODEL FIT TO OBSERVATIONS

The first diagnostic consists in a comparison of the model background coming from both experiments with radiosounding data (Fig. 15) for an area located between 65°S and the South Pole. The difference between observations and their counterparts derived from the model background (in our case, a 6-h range forecast), are the so-called innovations. The innovations are computed for each analysis time and statistics are accumulated over a 20-day period.

Results for temperature, zonal, and meridional winds are plotted in Fig. 15. These subplots show a better fit of the EXP background to radiosounding data than does the CONTROL. Best results are obtained in the lower troposphere. The rms of the difference between the observations and the background has decreased with the additional data for all parameters. A better fit, estimated through the rms, is also seen for other data, such as HIRS and Special Sensor Microwave Imager (SSM/I) observations (not shown). Improvements in EXP have been evaluated using a Student's *t* test (confidence level of 0.99), which indicates that the results are significant in the lower troposphere (pressure above 800 hPa) for the wind speed and the temperature. In the lower troposphere, the rms of wind speed has been improved by about 15% (e.g., in the layer 800–900 hPa, the rms has decreased from 5.17 to 4.7 m s^{-1}). For temperature, the most significant reduction of rms is for the layer 800–900 hPa, the mean rms has decreased from 0.7 to 0.04 K. Better statistics are seen together with an increase of data assimilated in the system.

The assimilation of additional data also has a positive impact at other latitudes, where the usage of data is less challenged. This is because of the propagation of the information by the assimilation cycling. Innovations calculated for a latitude band located between 20° and 60°S

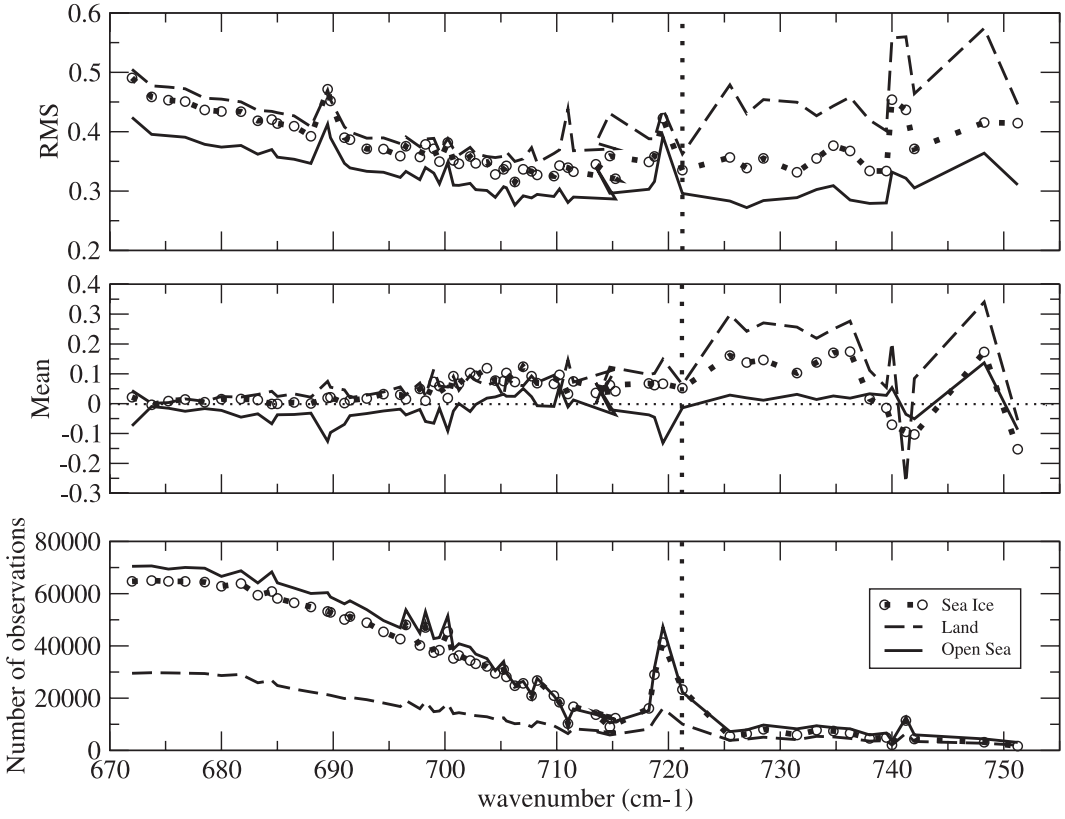

FIG. 12. The (top) rms and (middle) mean of innovations (after bias correction) as a function of the channel number for IASI for clear pixels for latitudes below 50°S for each surface type: land (dashed line), sea ice (dotted line with circle), and open sea (line). (bottom) The number of observations has been plotted as a function of the IASI channel number. The vertical dashed line indicates the thresholds on the channel number (x = 721.25 cm^{-1}).

show a better fit to aircraft report (AIREP) observations in EXP (measurements of the zonal and meridional wind components, and temperature at the flight level). For this latitude band, the AIREP observations are mainly available over Australia and New Zealand (see plot of AIREP tracks in Fig. 16). The corresponding aircraft innovation rms plots for these latitudes are presented at the bottom of Fig. 15. The rms of EXP innovations (black curve) is smaller than the rms of the CONTROL innovations (dashed curve) in the troposphere for zonal winds, meridional winds, and temperature components.

To continue the investigation, the quantification of the impact of the additional data, as a function of the latitude, through forecast error difference plots is illustrated in the next section.

2) AVERAGED FORECAST IMPACT

Forecasts have been run for EXP and CONTROL starting from the analysis at 0000 UTC each day, with a forecast range of 4 days. For both experiments, forecast errors have been computed with respect to ECMWF analyses, which provide an independent reference. Before commenting on the results, it is interesting to list the differences between the ECMWF channel selection and our experiment's channel selection for polar areas. In July 2007, the ECMWF's global model had a horizontal resolution of 25 km with 91 vertical levels. For AMSU-A, channel 14 is assimilated in ECMWF's global model compared to our experiments, this is due to the difference in the height of the top of the model in each meteorological center. Otherwise, ECMWF assimilates channels 5 and 6 over sea ice, as in the EXP experiment. For AMSU-B, as in the CONTROL experiment, a threshold on surface temperature is used, so no data are assimilated for temperatures below 278 K; therefore, almost no data are assimilated over Antarctica. For AIRS, over land, no data are assimilated for water vapor channels and short-wave channels. But more channels are used in long-wave channels. So this sampling is close to the EXP sampling but with less assimilated channels. Over open sea and sea ice, channels are assimilated for a wider frequency band: from long-wave channels, with water vapor channels to short-wave channels. For IASI, no channels are assimilated over land. Over sea ice and open sea, long-wave

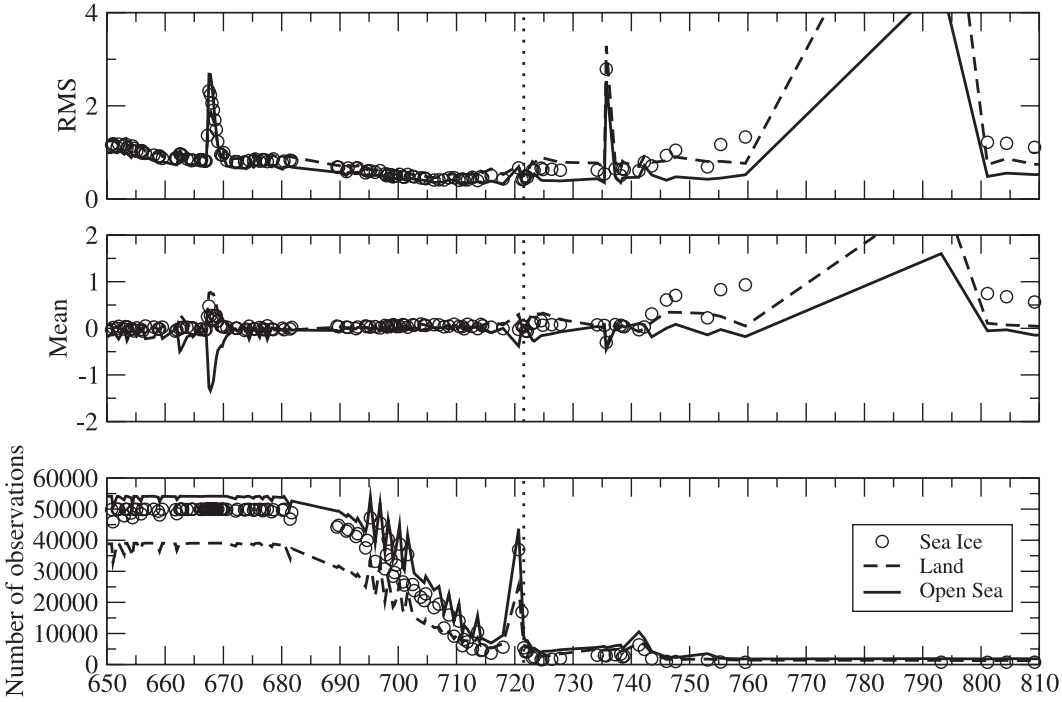

FIG. 13. As in Fig. 12, but for AIRS.

channels (not water vapor, nor shortwave) are assimilated. So, the channel selection at ECMWF is closer to the EXP channel selection than to the CONTROL over land. The main differences appear for the AMSU-B sensor and for IASI for which no data are assimilated over land. Over sea ice and open sea, more channels in a greater frequency band are assimilated for both infrared sensors AIRS and IASI.

Figure 17 shows statistics on the differences of the rms forecast error between CONTROL and EXP for the

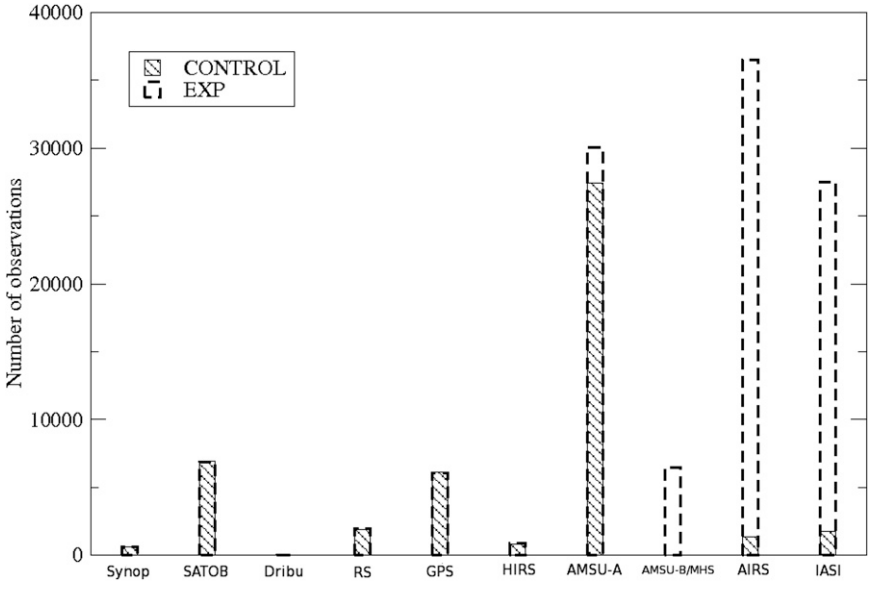

FIG. 14. Number of observations taken into account in the analysis for 10 observation types. (left to right) The list of observations: synop, SATOB, dribu, radiosounding (RS), GPS, HIRS, AMSU-A, AMSU-B/MHS, AIRS, and IASI. The shaded bars are for the CONTROL and the dashed bars for the EXP.

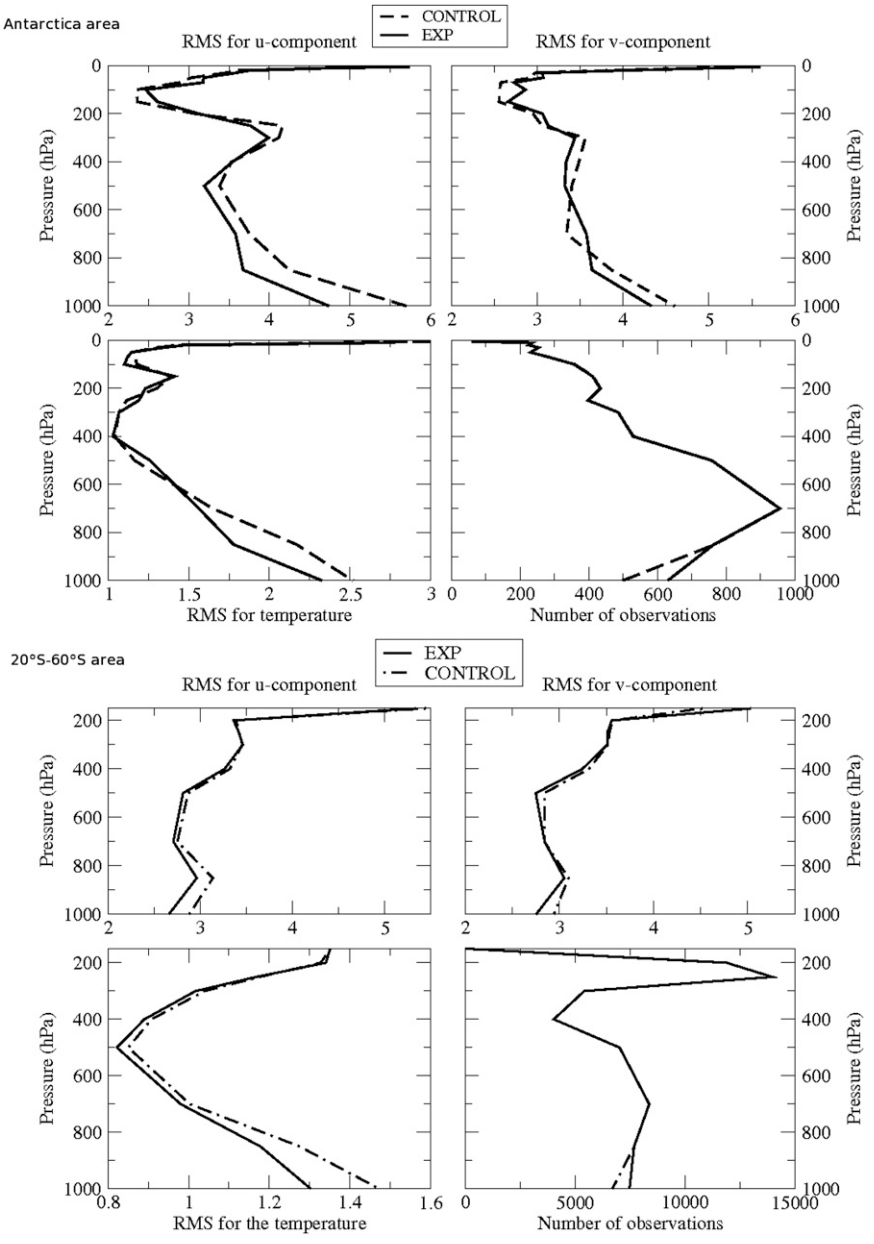

FIG. 15. Innovations (rms) and number of observations for EXP (solid line) and CONTROL (dashed line) for Antarctica area (latitudes below 65°S) on the top and same plot for latitudes between 20°S and 60° below. For Antarctica, the observations are radiosoundings and for the northern area, the observations are aircraft data (AIREP). For each area, four plots are done. The rms for (top left) the u component (m s^{-1}), (top right) the v component (m s^{-1}), (bottom left) the temperature, (bottom right) the number of observations are plotted in function of the pressure (on the y axis).

geopotential at four forecast steps (24, 48, 72, and 96 h). ECMWF analysis is set as the verifying analysis. Differences in forecast errors are computed and averaged over a 20-day period over July 2007. Blue (yellow) colors indicate that the EXP forecast has lower (larger) errors than the CONTROL forecast. This figure illustrates the positive impact, from a forecast point of view, of additional AIRS, IASI, and AMSU observations over Antarctica.

Improvement is seen at each forecast step for high latitudes with the largest of all between 200 and 500 hPa. The improvement seems to spread northward during the forecast (from 60° to 40°S). More experiments, which

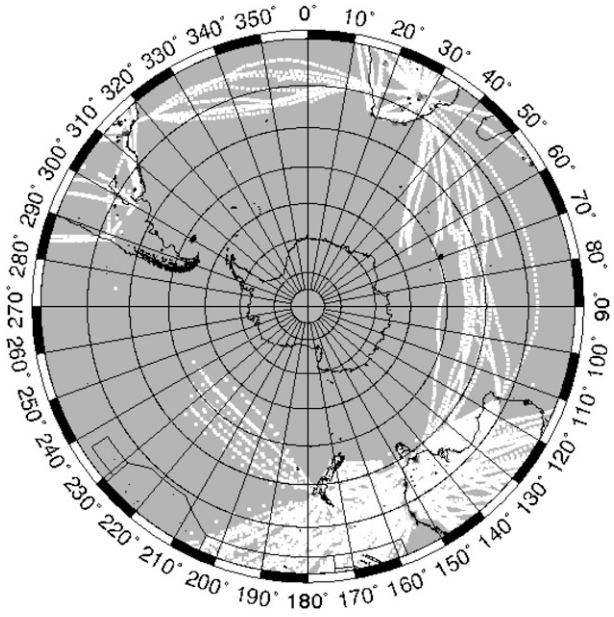

FIG. 16. AIREP tracks (white line) in the area between 20° and 60°S. Lines indicate the latitude and longitude every 10°.

assimilate either additional microwave or infrared data, have shown that although all data contribute to this improvement, microwave data seem to bring the largest positive impact. Finally, yellow contours associated with a forecast degradation are seen in the lower atmosphere (below 700 hPa), for latitudes below 80°S. This result must to be run with the orography of this area in mind. For this part of Antarctica (see Fig. 2), the orography is very high and, as a consequence, few AMSU data are assimilated. Moreover, it is important to recall that infrared sensors are assimilated only from the stratosphere to the midtroposphere.

3) IMPACT ON THE MEAN SNOW PRECIPITATION

A good knowledge of the amount of the snow precipitation for polar areas is of prime importance for meteorology and climate. Averages of a 24-h accumulated snow precipitation have been estimated for EXP and CONTROL for the entire assimilation period. Differences can reach 0.2 mm on the coast where the average precipitation is about 0.5–1 mm. These differences can reach 20%, which is far from being negligible. Maps of the temperature difference also show major differences over the coast located near the same place as the extrema of accumulated snow difference. In Fig. 18, the average of mean accumulated snow precipitation has been plotted against longitude ranges for both CONTROL and EXP experiments. Overall, EXP forecast produces more snow precipitation for all latitudes, with a peak of snow precipitation between 60° and 70°S.

Other mean fields (e.g., temperature and specific humidity) have been plotted for both experiments to understand this increase. The magnitude of the field differences is greater at the initial time than at the 24-h forecast time. During the forecast, the differences tend to decrease. At the initial time, an excess of specific humidity is detected over Antarctica for the EXP experiment. To regulate it, the model precipitates this excess of specific humidity. The decrease of the specific humidity in EXP is then faster than in CONTROL. This transformation of the specific humidity is confirmed by the increase in temperature. It should be recalled that the condensation process is tied to an increase of temperature. Moreover, the comparison of the different precipitation types (i.e., large scale, convective, snow, rain) indicates that the signal in the snow precipitation presented in this section mainly comes from the large-scale snow precipitation. A convective part of the snow precipitation appears near the latitude 60°S. At the end of the forecast, the two experiments tend toward the same state. At the 96-h forecast range, the impact of the data assimilation has almost disappeared from a precipitation point of view.

c. *Case study*

The time evolution of the forecast error for EXP and CONTROL has been calculated over the study period. The two experiments are compared for the geopotential at the 72-h forecast range in two areas: the whole Southern Hemisphere (20°S) and the Australia–New Zealand area. The rms of EXP is smaller than the rms of CONTROL for many days (e.g., during the period from 23 to 27 July 2007). For this parameter, no change is seen over the Australia–New Zealand area. Consequently, the improvement in the rms is presumably due to changes over Antarctica, because for the area south of 20°S, radiosoundings are mainly located over the Australia–New Zealand area and over Antarctica. It is interesting to note that the radiosoundings are mainly located over the coast of Antarctica where most disturbances take place. Based on this preliminary analysis, the date of 26 July 2007 has been chosen as a case study. The forecast of the 23 July 2007 for both experiments will be compared to the ECMWF analysis (3 days later).

1) GEOPOTENTIAL

Previous studies have shown that the mean sea level pressure (MSLP) is not a good variable to be considered over Antarctica because of the orography of this continent, especially over the eastern part where mountains can reach a 4-km height. The geopotential height at 500 hPa has been chosen instead of MSLP as the relevant

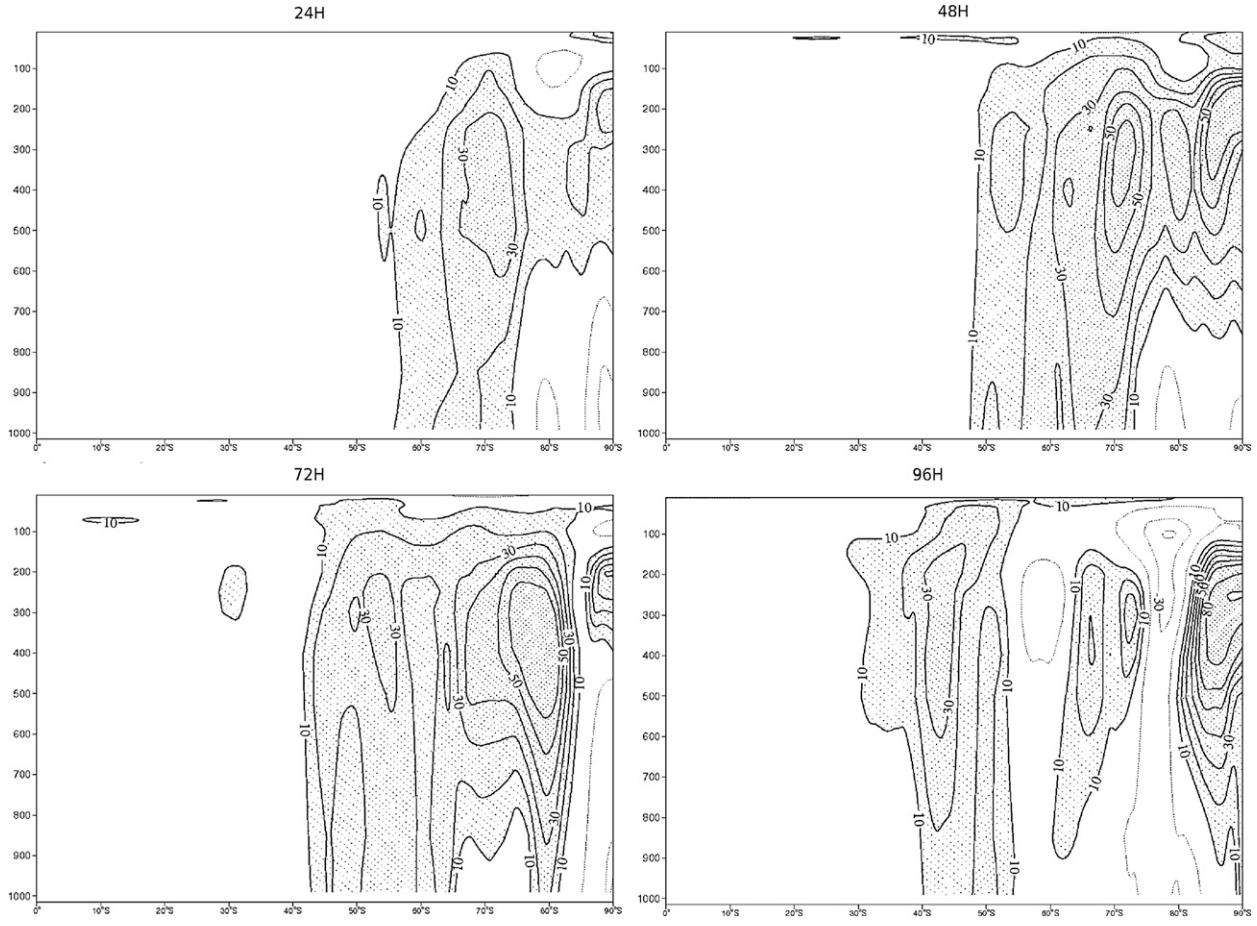

FIG. 17. Statistics of the differences in rmse between a version of the ARPEGE model assimilating the same observations as in operations and a version of the model using more satellite data over Antarctica. The statistics are shown for the geopotential errors of the (top left) 24-, (top right) 48-, (bottom left) 72-, and (bottom right) 96-h forecasts over a period of 3 weeks in July 2007 averaged longitudinally. The vertical scale is pressure and the horizontal scale is latitude. Solid line (dotted line) indicates that the additional AIRS, IASI, and AMSU observations over Antarctica have improved (degraded) the forecasts.

parameter to document the atmospheric flow (Turner and Pendlebury 2004; Pendlebury et al. 2003).

Maps of geopotential at 500 hPa are plotted for Antarctica for CONTROL and EXP experiments at the 72-h forecast range (Fig. 19, subplots A, B, and C). The ECMWF analysis is used as reference. In Fig. 19, three geopotential minima are visible in the analysis (top left, A). They are located at 1 (60°S, 180°), 2 (65°S, 50°W), and 3 (60°S, 10°E). The comparison between EXP forecast (bottom, C) and the CONTROL (top right, B), indicates a better forecast of these features in EXP. Maps of differences between EXP forecast and the analysis (on the right-hand side, E) and CONTROL forecast and the analysis (on the left-hand side, D) are shown below. Forecast errors have decreased quite remarkably as seen, for example, near the longitude 65°E. Two others maps of difference are also shown in the lower part of the figure. These maps show the impact of the additional infrared (on the left-hand side, figure F) and microwave (on the right-hand side, figure G) when these satellite data are assimilated independently. These maps illustrate the relative impact of infrared and microwave data. For both cases, the errors between forecast and analysis are decreasing with additional data. The assimilation of more microwave data leads to a bigger impact in the decrease of the forecast error.

The correlation coefficient between the 72-h forecast from CONTROL (EXP) and the analysis has been estimated for the geopotential at 500 hPa. A mean correlation value of 0.97 is found for EXP compared with a mean correlation value of 0.93 for CONTROL. A similar improvement has been found when deriving correlations for other dates (e.g., for the analysis of 24 July 2007). The EXP forecast, compared to an independent analysis, is found to be better than CONTROL, in terms of both rms errors and correlations.

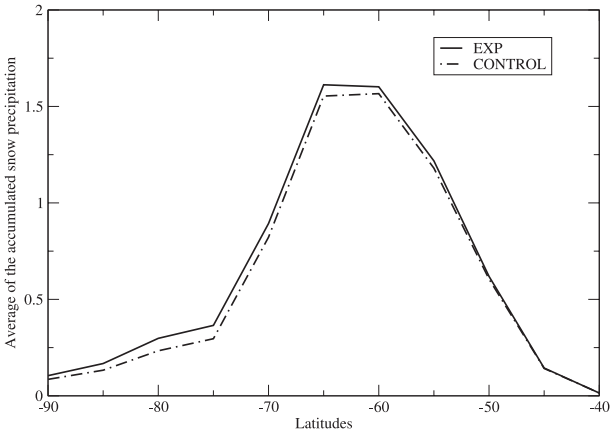

FIG. 18. Average over the longitudes of the mean accumulated snow precipitation (mm) for the 24-h forecasts over 20 days in July 2007. The solid line is for the EXP and the dashed line for the CONTROL.

2) SNOW PRECIPITATION

Besides the geopotential field, which illustrates the general circulation, it seems purposeful to compare other derived fields which are also relevant for Antarctica. The total precipitation of snow accumulated over 3 days since the 23 July 2007 is investigated. Maps of this field are shown in Fig. 20 for the ECMWF model and the EXP and CONTROL experiments. The difference in accumulated precipitation between both experiments (EXP − CONTROL) has also been calculated. The main differences are located over the Antarctica coast and South America, between 70° and 50°S, in an area of low pressure systems. If this figure is compared with Fig. 19 for geopotential, the extrema of precipitation differences coincide with the three geopotential minima highlighted earlier. The comparison between EXP and CONTROL forecasts for geopotential reveals that EXP forecast give a better prediction of the position of these minima. Figure 20 shows that, in these disturbances, EXP predicts more snow precipitation. Moreover, if we compare the results for EXP and CONTROL with ECMWF, the amount of snow precipitation estimated using ECMWF is lower than in EXP and CONTROL experiments, but the extrema present in all experiments are located in same area, which is coherent with the geopotential field (see previous section). The comparison between ECMWF and experiments has shown that the main difference is located near the three geopotential minima. One should note that similar results have been found when infrared and microwave data are separately assimilated.

4. Discussion

Developments have been tested in order to increase the number of assimilated satellite observations from both microwave and infrared sensors over Antarctica and the sea ice surroundings. The method developed by Karbou et al. (2006) to estimate microwave emissivity from satellite observations has been applied and adjusted for cold areas (land and sea ice). This modification of the surface emissivity has improved innovation statistics, which implies that the simulation of brightness temperatures from model fields was in better agreement with observations. Therefore, the assimilation of additional AMSU-A/B data has been performed over Antarctica and sea ice. In parallel, the use of IASI and AIRS data has been extended over snow and sea ice, once the statistics have been proven to be satisfactory. This extended use of data has led to positive results in terms of assimilation and forecast. Indeed, it was found that the increase in the number of observations had a positive impact on the analysis and on the forecast, for a model especially tuned for Antarctica. The forecast impact was found to affect the snow precipitation amount around Antarctica and to propagate to lower latitudes during the forecast. This version of the ARPEGE model will be helpful for meteorological forecasts during the second phase of the Concordiasi campaign in 2010, when stratospheric balloons will bring information both at the gondola level (around 60 hPa) and by dropping sondes. These sondes will be dropped according to IASI overpasses. Specific studies based on these new soundings will then be performed in order to improve the understanding of data assimilation for cold surfaces.

For land emissivity modeling, physical assumptions were reconsidered over snow (Guedj et al. 2009). The authors have studied the effect of assumptions about the surface on calculated emissivities over Antarctica. It was found that the use of a Lambertian approximation for AMSU is more suitable during winter whereas the specular assumption can be used during summer. Another way to improve the emissivity calculation, and consequently the microwave data assimilation, could be to evaluate more accurately the surface temperature. Karbou et al. (2006) has tested an approach for the surface temperature calculation in a 4D-Var system. Following the same idea as for the emissivity, surface temperature can be calculated from satellite observations at one surface channel and then affected to other channels, with an emissivity taken from an atlas. These approaches are going to be the focus of further research.

To improve the infrared data assimilation, studies on cloud detection could also be performed. Different cloud detection methods could be tested over Antarctica and compared to the current ECMWF method developped by McNally and Watts (2003). Other methods such as the CO_2-slicing method (Chahine 1974; Lavanant 2002; Pangaud et al. 2009) or the Multivariate Minimum

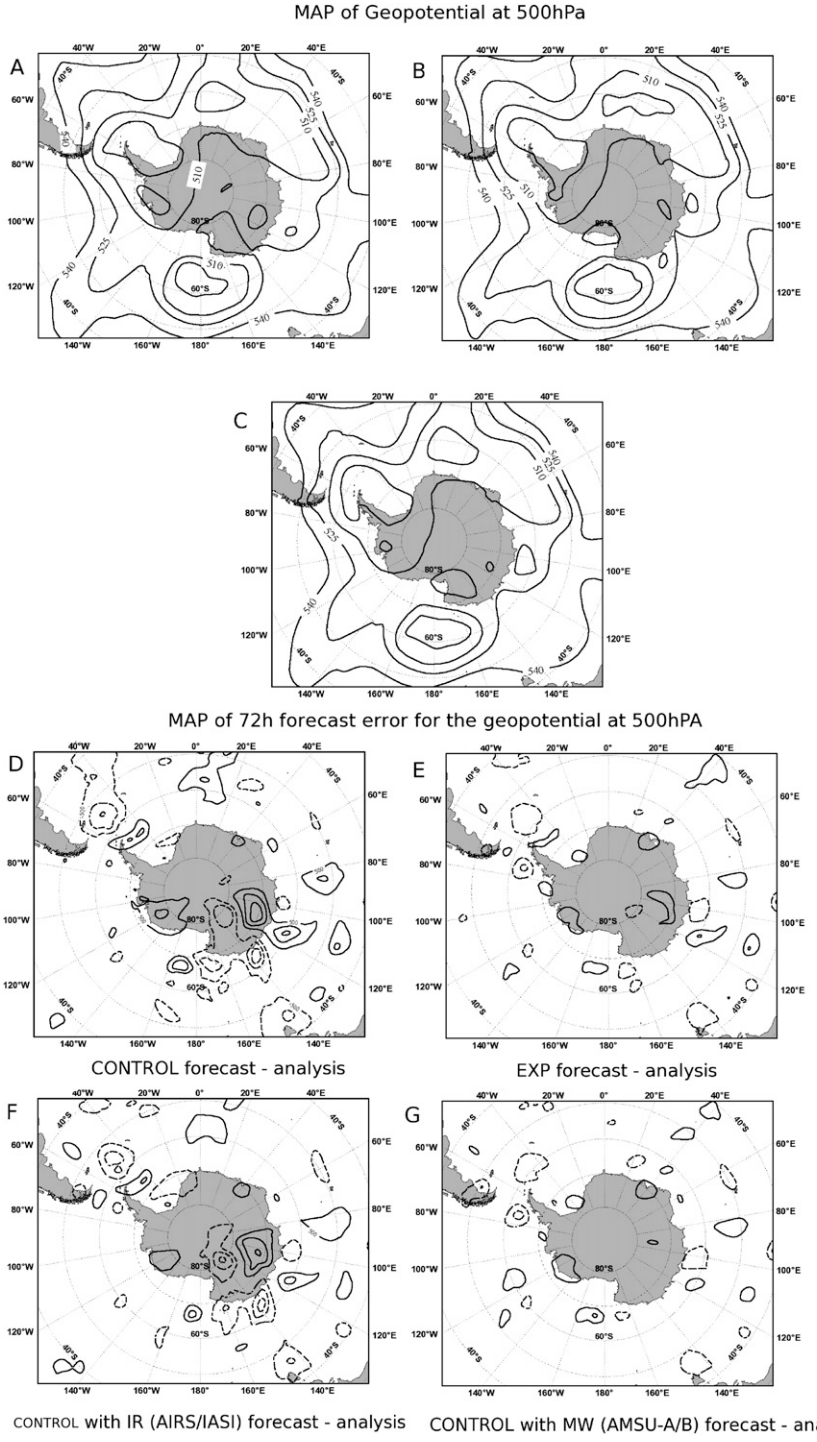

FIG. 19. (top) Maps of geopotential at 500 hPa (unit: × 100 m). The first one is the analysis of ECMWF. The second is an output at the forecast of 72 h for the CONTROL, and the last one is the 72-h forecast for the EXPERIMENT. Date of the analysis: 26 Jul 2007. Isolines each 1500 from 51 000 to 55 000 m. (bottom) Map of 72-h forecast errors for the geopotential at 500 hPa. (top left) Difference between the CONTROL forecast and the analysis. (top right) Difference between the EXP forecast and the analysis. (bottom left) Difference between the CONTROL with infrared sensors (AIRS and IASI) forecast and the analysis. (bottom right) Difference between the CONTROL with microwave sensors (AMSU-A/B) forecast and the analysis. The date of the analysis is 26 Jul 2007. Isolines each 500 m from −2000 to 2000 m.

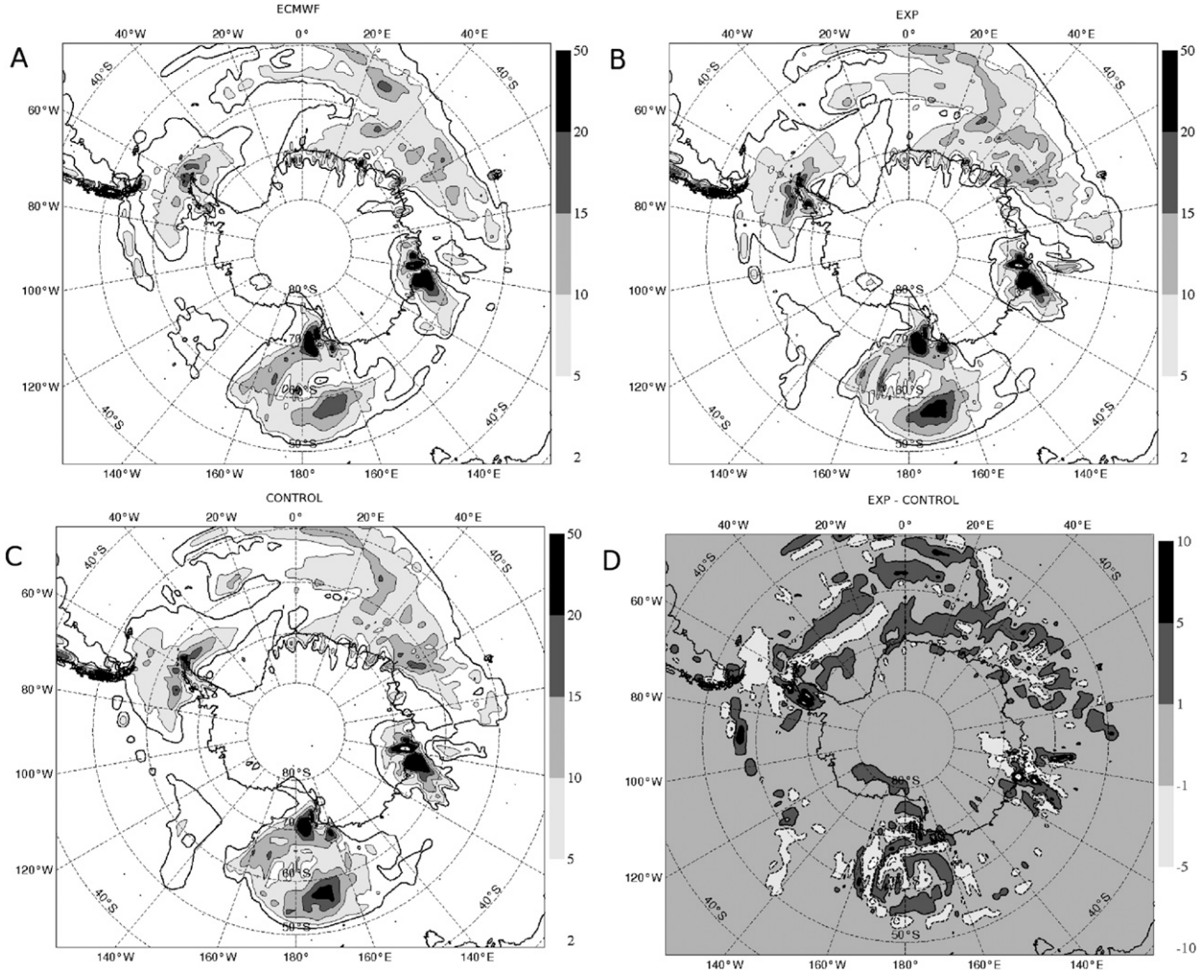

FIG. 20. Maps of the snow precipitation amount over 3 days between the forecast at 72 h for (top left) ECMWF, (top right) EXP, and (bottom left) CONTROL. (bottom right) Difference of the snow precipitation amount over 3 days between the forecast at 72 h of the EXP and the CONTROL. (Date of analysis: 26 Jul 2007).

Residual Method (MMR) could be tried (Auligne 2007). However, the validation of a given method of cloud detection, with satellite data, is very difficult over the Poles. Imagers such as MODIS can supply information on the cloud-top pressure or the cloud fraction, but the error tied to these products is bigger over cold surfaces. One possibility would be to investigate the use of sensors on the A-train or visual observations over Antarctica to perform more local comparisons.

Work on infrared and microwave data assimilation will be carried on along the directions indicated above, using additional in situ data obtained during the Concordiasi experiment as validation. Although this research has been performed in the context of the French NWP system, the methods could be used in different systems and the results are believed to be general.

Acknowledgments. Concordiasi was built by an international scientific group and is currently supported by the following agencies: Météo-France, CNES, IPEV, PNRA, CNRS/INSU, NSF, UCAR, University of Wyoming, Purdue University, University of Colorado, and ECMWF. The two operational polar agencies PNRA and IPEV are thanked for their suppport at Concordia station and at the coast of Adelie Land. The NSF is thanked for its support at the McMurdo base. Concordiasi is part of the THORPEX-IPY cluster within the International Polar Year effort. Detailed information on Concordiasi is available online at http://www.cnrm.meteo.fr/concordiasi/. Acknowledgments are given to the French Centre National d'Etudes Spatiales (CNES) for their financial support. The authors thank Jean Maziejewski for his help revising the manuscript. We

would also like to acknowledge two anonymous reviewers for helping to substantially improve the manuscript.

REFERENCES

Adams, N., 1997: Model prediction performance over the Southern Ocean and coastal region around east Antarctica. *Aust. Meteor. Mag.,* **46,** 287–296.

Auligne, T., 2007: Variational assimilation of infrared hyperspectral sounders data: Bias correction and cloud detection. PHD thesis, University Paul Sabatier, 222 pp.

——, A. McNally, and D. Dee, 2007: Adaptative bias correction for satellite data in a numerical weather prediction system. *Quart. J. Roy. Meteor. Soc.,* **133,** 631–642.

Barker, D. M., 2005: Southern high-latitude ensemble data assimilation in the Antarctic mesoscale prediction system. *Mon. Wea. Rev.,* **133,** 3431–3449.

Belo Pereira, M., and L. Berre, 2006: The use of an ensemble approach to study the background error covariances in a global NWP model. *Mon. Wea. Rev.,* **134,** 2466–2489.

Bromwich, D. H., R. I. Cullather, and R. Grumbine, 1999: An assessment of the NCEP operational global spectral model forecasts and analyses for Antarctica during frost. *Wea. Forecasting,* **14,** 835–850.

Chahine, M. T., 1974: Remote sounding of cloudy atmospheres. Part I: The single cloud layer. *J. Atmos. Sci.,* **31,** 233–243.

Comiso, J. C., 2000: Variability and trends in Antarctic surface temperatures from in situ and satellite infrared measurements. *J. Climate,* **13,** 1674–1695.

Courtier, P., and J.-F. Geleyn, 1988: A global numerical weather prediction model with variable resolution: Application to the shallow-water equations. *Quart. J. Roy. Meteor. Soc.,* **114,** 1321–1346.

——, C. Freydier, J.-F. Geleyn, F. Rabier, and M. Rochas, 1991: The ARPEGE project at Météo France. *Proc. ECMWF Workshop on Numerical Methods in Atmospheric Modelling,* Vol. 2, Reading, United Kingdom, ECMWF, 193–231.

——, J. N. Thpault, and A. Hollingsworth, 1994: A strategy for operational implementation of 4D-VAR, using an incremental approach. *Quart. J. Roy. Meteor. Soc.,* **120,** 1367–1387.

Cullather, R. I. D., H. Bromwich, and R. W. Grumbine, 1997: Validation of operational numerical analyses in Antarctic latitudes. *J. Geophys. Res.,* **102,** 13 761–13 784.

Dahoui, M., L. Lavanant, F. Rabier, and T. Auligne, 2005: Use of the MODIS imager to help deal with AIRS cloudy radiances. *Quart. J. Roy. Meteor. Soc.,* **131,** 2559–2579.

Deblonde, G., and S. J. English, 2000: Evaluation of the FASTEM-2 fast microwave oceanic surface emissivity model. *Proc. 11th Int. ATOVS Study Conf.,* Budapest, Hungary, 67–78.

English, S. J., 1999: Estimation of temperature and humidity profile information from microwave radiances over different surface types. *J. Appl. Meteor.,* **38,** 1526–1541.

——, 2008: The importance of accurate skin temperature in assimilating radiances from satellite sounding instruments. *IEEE Trans. Geosci. Remote Sens.,* **46,** 403–408.

Eyre, J., 1991: A fast radiative transfer model for satellite sounding systems. ECMWF Tech. Memo. 176, 28 pp. [Availabale from ECMWF, Shinfield Park, Reading, Berkshire RG2 9AX, United Kingdom.]

Goldberg, M., Y. Qu, L. McMillin, W. Wolf, L. Zhou, and M. Divarkarla, 2003: AIRS near-real-time products and algorithms in support of operational numerical weather prediction. *IEEE Trans. Geosci. Remote Sens.,* **41,** 379–389.

Grody, N. C., 1988: Physical retrieval of land surface temperature using the Special Sensor Microwave Imager. *J. Geophys. Res.,* **103,** 8839–8848.

Guedj, S., F. Karbou, F. Rabier, and A. Bouchard, 2009: Toward a better modeling of surface emissivity to improve AMSU data assimilation over Antarctica. *IEEE Trans. Geophys. Remote Sens.,* in press.

Hewison, T., and S. English, 2000: Fast models for land surface emissivity. Cost Action 712—Radiative transfer models for microwave radiometry, Final Rep. of Project 1, EUR19543EN, European Commission, 117–127.

Jourdan, N., 2007: Regional climatic simulation coupled atmosphere-ocean-sea ice in Antarctica. PHD. thesis. University Joseph Fourrier, 173 pp.

Kalnay, E., D. J. Lord, and R. D. McPherson, 1998: Maturity of operational numerical weather prediction: Medium range. *Bull. Amer. Meteor. Soc.,* **79,** 2753–2769.

Karbou, F., E. Gerard, and F. Rabier, 2006: Microwave land emissivity and skin temperature for AMSU-A and -B assimilation over land. *Quart. J. Roy. Meteor. Soc.,* **132,** 2333–2355.

——, ——, and ——, 2010: Global 4DVAR assimilation and forecast experiments using AMSU observations over land. Part I: Impact of various land surface emissivity parameterizations. *Wea. Forecasting,* **25,** 5–19.

King, J. C., and J. Turner, 1997: *Antarctic Meteorology and Climatology*. Cambridge University Press, 409 pp.

Lavanant, L., 2002: Cloud processing in IASI context. *Proc. 12th Int. ATOVS Study Conf.,* Lorne, Australia, ATOVS, 8 pp.

Leonard, S., J. Turner, and S. Milton, 1997: An assessment of U.K. Meteorological Office numerical weather prediction analyses and forecasts for the Antarctic. *Antarct. Sci.,* **9,** 100–109.

Mathew, N., 2007: Retrieval of surface emissivity of sea ice and temperature profiles over sea ice from passive microwave radiometers. Berichte aus dem Institut fur Umweltphysik, Band 35, 126 pp.

Matricardi, M., F. Chevallier, G. Kelly, and J. Thépaut, 2004: Channel selection method for IASI radiances. *Quart. J. Roy. Meteor. Soc.,* **130,** 153–173.

McNally, A. P., 2007: The use of satellite data in polar regions. *Seminar Proc.,* Reading United Kingdom, ECMWF, 12 pp.

——, and P. D. Watts, 2003: A cloud detection algorithm for high spectral resolution infrared sounders. *Quart. J. Roy. Meteor. Soc.,* **129,** 3411–3423.

Nordeng, T. E., G. Brunet, and J. Caughey, 2007: Improvement of weather forecasts in polar region. WMO Bull., International Polar Year 2007–2008, 7 pp.

Pangaud, T., N. Fourrie, V. Guidard, M. Dahoui, and F. Rabier, 2009: Assimilation of AIRS radiances affected by mid- to low-level clouds. *Mon. Wea. Rev.,* **137,** 4276–4292.

Pendlebury, S. F., N. D. Adams, T. L. Hart, and J. Turner, 2003: Numerical weather prediction model performance over high southern latitudes. *Mon. Wea. Rev.,* **131,** 335–353.

Picard, G., L. Brucker, M. Filly, H. Galle, and G. Krinner, 2009: Modeling time series of microwave brightness temperature in Antarctica. *J. Glaciology,* **55,** 537–551.

Powers, J. G., 2007: Numerical prediction of an Antarctic severe wind event with the Weather Research and Forecasting (WRF) model. *Mon. Wea. Rev.,* **135,** 3134–3157.

Rabier, F., H. Järvinen, E. Klinker, J.-F. Mahfouf, and A. Simmons, 2000: The ECMWF operational implementation of four-dimensional variational assimilation. I: Experimental results with simplified physics. *Quart. J. Roy. Meteor. Soc.,* **126,** 1143–1170.

——, and Coauthors, 2007: The Concordiasi Project over Antarctica during the International Polar Year (IPY). *Proc. Joint EUMETSAT/AMS Conf.,* Amsterdam, Netherlands, 8 pp.

——, and Coauthors, 2010: The Concordiasi Project in Antarctica. *Bull. Amer. Meteor. Soc.,* **91,** 69–86.

Saunders, R. W., M. Matricardi, and P. Brunel, 1999: An improved fast radiative transfer model for assimilation of satellite radiance observations. *Quart. J. Roy. Meteor. Soc.,* **125,** 1407–1425.

Semane, N., 2008: Study by simulation and assimilation of the chemistry composition and exchanges in the high troposphere-low stratosphere. PHD. thesis, University Paul Sabatier, 160 pp.

Solomon, S., D. Qin, M. Manning, M. Marquis, K. Averyt, M. M. B. Tignor, H. L. Miller Jr., and Z. Chen, Eds., 2007: *Climate Change 2007: The Physical Sciences Basis*. Cambridge University Press, 996 pp.

Trigo, I. F., and P. Viterbo, 2003: A comparison between observations and the ECMWF model. *J. Appl. Meteor.,* **42,** 1463–1479.

Turner, J., and S. Pendlebury, 2004: *The International Antarctic Weather Forecasting Handbook*. British Antarctic Survey, 685 pp.

——, and Coauthors, 2005: Antarctic climate change during the last 50 years. *Int. J. Climatol.,* **25,** 279–294.

Wee, T.-K., and Y.-H. Kuo, 2004: Impact of a digital filter as a weak constraint in MM5 4D-VAR: An observing system simulation experiment. *Mon. Wea. Rev.,* **132,** 543–559.

——, and ——, 2008: Assimilation of GPS radio occulation refractivity data from CHAMP and SAC-C missions over high southern latitudes with MM5 4DVAR. *Mon. Wea. Rev.,* **136,** 2923–2944.

Weng, F., and B. Yan, 2003: A microwave snow emissivity. *Proc. 13th Int. ATOVS Study Conf.,* Saint-Adele, Canada, 8 pp.